6-1-2012

Networked control systems for intelligent transportation systems and industrial automation

Tarek Khaled Salaheldin Ismail Refaat

Follow this and additional works at: https://fount.aucegypt.edu/etds

Recommended Citation

APA Citation

Refaat, T. (2012). *Networked control systems for intelligent transportation systems and industrial automation* [Master's thesis, the American University in Cairo]. AUC Knowledge Fountain.
https://fount.aucegypt.edu/etds/1237

MLA Citation

Refaat, Tarek Khaled Salaheldin Ismail. *Networked control systems for intelligent transportation systems and industrial automation*. 2012. American University in Cairo, Master's thesis. *AUC Knowledge Fountain*.
https://fount.aucegypt.edu/etds/1237

The American University in Cairo

School of Sciences and Engineering

NETWORKED CONTROL SYSTEMS
FOR INTELLIGENT TRANSPORTATION SYSTEMS
AND INDUSTRIAL AUTOMATION

A Thesis Submitted to

The Electronics Engineering Department

in partial fulfillment of the requirements for
the degree of Master of Science

by Tarek Khaled Salaheldin Ismail Refaat

under the supervision of Prof. Hassanein H. Amer and Dr. Ramez M. Daoud
May/2012

i

Approval Sheet Goes Here

DEDICATION

I dedicate this thesis to my dear Mother and Father for their limitless and transcendent support. I also dedicate it to my siblings, in hopes that some day they would surpass any achievement they hold dear to them. I also wish to include several dear family members for their roles in making me who I am today.

Mom: Your endless Faith in me has made me who I am, never aiming lower than the stars.

Dad: I cannot put into words how selflessly you have sacrificed to support me throughout the past. You have chosen to leave my siblings and I as your legacy to this world, and here I am, hopefully in some small part, a testimony to you that - You have succeeded and it was worth it.

I would like to dedicate this thesis in no small part to Prof. Hassanein Amer and Prof. Ramez M. Daoud. You both have been my father and elder brother for the past years and I can never quantify my appreciation for your support. I guarantee I shall forever hold you both in my highest regard. You have both shown me what it means to be teachers and mentors. Standing in the highest rank of integrity and purity. Thank you both.

I must also mention Mrs. Amal Khouzam and my youngest brother, the youngest person to enter the research lab! I hope to hear nothing but the best about you both in future! God bless you both.

Last but of course not least, Prof. Amani ElGammal, who put me on the first step of this wonderful career. I cannot thank you enough for your support throughout my academic life.

I wish to thank all my dear friends, old and new, especially Karam, Seemi and Ziyad, for their support and faith in me along the way. I'd mention everyone else, but I've only got one page guys.

Special mention goes to my dear students: You know who you are. You'd better stay in touch!

May Allah grant you all happiness in this life and the next.

ACKNOWLEDGMENTS

TABLE OF CONTENTS

LIST OF FIGURES

LIST OF TABLES

LIST OF ABBREVIATIONS

NCS	Networked Control System
WNCS	Wireless Networked Control System
S	Sensor
A	Actuator
SAs	Sensors &/or Actuators
K	Controller (or Control Server)
E	Entertainment Server
AP	Access Point
WISA	Wireless Interface for Sensors and Actuators (by ABB)
CAN	Controller Area Network
CSMA/CD	Carrier Sense Multiple Access with Collision Detection
CSMA/CA	Carrier Sense Multiple Access with Collision Avoidance
BEB	Binary Exponential Backoff
SSP	Steady-State Performability
TP	Transient Performability
CP	Cumulative Performability
ITS	Intelligent Transportation Systems
IA	Industrial Automation
TMR	Triple Modular Redundancy
GbE	Gigabit Ethernet
ISM	Industrial, Scientific and Medical
UDP	User Datagram Protocol
TCP	Transmission Control Protocol
BSS	Basic Service Set
PRPT	Packet-Reception-Power-Threshold
SSID	Service Set Identifier
FT	Fault-Tolerance/Fault-Tolerant
FF	Fault-Free
CTMC	Continuous Time Markov Chain
IP	Internet Protocol

ABSTRACT

The American University in Cairo, Egypt

Networked Control Systems for Intelligent Transportation Systems
and Industrial Automation

Name: Tarek Khaled Salaheldin Ismail Refaat

Supervisors: Prof. Hassanein H. Amer, Dr. Ramez M. Daoud

This thesis presents a study of two different applications of Networked Control Systems:

Ethernet Networked Control System On-board of Train-wagons:
An Ethernet backbone is shared between control and entertainment. The wagon contains a dedicated control server and a dedicated entertainment server, which act as fault-tolerant machines for one another. In the event of a server failure, the remaining machine can serve both entertainment and/or control. The study aims at enhancing system design in order to maximize the tolerable entertainment load in the event of a control/entertainment server failure, while not causing any control violations. This fault-tolerant system is mathematically analyzed using a performability model to relate failure rates, enhancements and rewards.

The model is taken further to test two identical wagons, with a total of four fault-tolerant servers. All possible failure sequences are simulated and a different communication philosophy is tested to further minimize the degradation of the entertainment load supported during the failure of up to three of the four servers. The system is shown to be capable of operating with minimal degradation with one out of four servers.

Wireless Networked Control Systems (WNCS) for Industrial Automation:
A WNCS using standard 802.11 and 802.3 protocols for communication is presented. Wireless Interface for Sensors and Actuators (WISA) by ABB is used as a benchmark for comparison. The basic unit is a single workcell, however, there is a need to cascade several cells along a production line. Simulations are conducted and a nontraditional allocation scheme is used to ensure correct operation under the effect of co-channel interference and network congestion. Next, fault-tolerance at the controller level is investigated due to the importance of minimizing downtime resulting from controller failure. Two different techniques of interconnecting neighboring cells are investigated. The study models both a two and three-cell scenario, and all systems show that fault-tolerance is achievable. This is mathematically studied using a performability analysis to relate failure rates with rewards at each failure state.

All simulations are conducted on OPNET Network Modeler and results are subjected to a 95% confidence analysis.

1. INTRODUCTION

At this time, the field of Networked Control Systems (NCS) is one that can be characterized as a niche in the academic world. There are few to no courses and/or formal references that address the field. The field is spearheaded by researchers in industry rather than academia. Research topics under the heading of NCS can be described as a point on a wide spectrum, ranging from pure control theory to pure networking. The applications of NCS also vary greatly, from Industrial Automation to Intelligent Transportation Systems, and the impact of such applications is far-reaching. Unlike communications or electromagnetics, the applications of NCS are far less visible to the common consumer's eye and hence many are unaware of the extent of its importance. This study addresses two different but interrelated applications of NCS. Each of the two applications has its own background and will be addressed in a separate section of the survey.

Section 2 starts with a literature survey of networked Control Systems in general. Then, fault-tolerance and Performability are addressed as these concepts will be used in both applications of NCS, namely, Intelligent Transportation Systems and Wireless NCS (WNCS) for Industrial Automation. More details are then presented regarding previous work in the area of ITS. WNCS for Industrial Automation existing solutions are then surveyed with a focus on a system proposed by ABB. The section ends with the problem statement.

Section 3 presents the author's contribution in the area of ITS. It starts with a single train wagon model and its fault-tolerant architecture. Enhancements of this architecture are then discussed and a Performability analysis is presented. Failure sequence permutations for a two train wagon model are then investigated in the context of two train wagons.

Section 4 focuses on WNCS for Industrial Automation. This work is based mainly on a system proposed by ABB. It will be shown how to achieve concatenation at 0m by using a special channel allocation scheme. Fault-tolerance is then studied in the context of two cells. Finally, an architecture based on 802.11g is developed and analyzed. A performability model with a novel reward scheme, is presented.

The thesis is concluded in Section 5.

2. LITERATURE SURVEY

2.1.   NETWORKED CONTROL SYSTEMS (NCS)

Networked control systems share certain aspects across the range of different applications. Typically, a NCS is composed of Sensors (S), Actuators (A) and a Controller (K). Sensors sample data from the plant (the physical system) and this data is sent to the controller. The controller, after some processing, makes a decision and sends this decision to the actuator, which applies the decision to the plant. The existence or lack thereof of a clock signal, determines whether the system is time-triggered (or clock-driven) or event-triggered. A clock-driven system consists of sensors and actuators (SAs) with constant sampling periods and samples are taken at discrete time points, whereas an event-triggered system has continuous sampling and an event triggers the control process [1]. The time taken by a packet to travel from S to K and K to A respectively (propagation/transmission delays) may or may not include processing time, encapsulation, decapsulation and queuing delays, depending on the system design.

NCS applications are characterized into real-time and non-real-time. Real-time applications of NCS typically involve small, frequently exchanged packets [2, 3]. The number of packets, their rate, the criticality of the data and the tolerable losses determine the sub-categorization between hard and soft real-time systems, the latter being able to tolerate more delays and more losses [4–6].

Unlike networks of today, NCS pioneers favored determinism and predictability of performance. Protocols such as Controller Area Network (CAN) and PROFIBUS served these aspects, highly deterministic and refined protocols, used for the majority of NCS applications [7–11]. However, with the natural demand for higher bandwidth and accessibility, more robust and non-deterministic protocols such as Ethernet made their way into the world of real-time NCS [2, 12–17]. Among the sources of randomness, which stood against the use of Ethernet for real-time NCS applications, is the utilization of Carrier Sense Multiple Access with Collision Detection (CSMA/CD) [10]. This multiple access technique employs the concept of Binary Exponential Backoff (BEB), whereby a transmitting node 'backs off' from transmission upon detection of a collision. The duration for this backoff is a value

between 0 and $2^k - 1$ time-slots, where k is the number of collisions detected/avoided, the duration growing exponentially as the number of collisions increases. To decrease the effect of this randomness, several modifications were made to the Ethernet standard, specifically to accommodate real-time applications. These modifications include (but not limited to) EtherNet/IP, Time-Triggered Ethernet (TT Ethernet) and Flexible TT Ethernet (FTT Ethernet) [18–25]. Recently unmodified Ethernet for use in real-time applications has been standardized [27, 28].

2.2. FAULT-TOLERANCE AND PERFORMABILITY

Fault-tolerance is a hot-topic in many research fields, due to the advantages of a fault-tolerant system over a normal system. As the term indicates, a fault-tolerant system is one that can 'tolerate' a fault in one or more aspects/components. The system can continue operation, maybe with degraded performance, but will not fail completely [28–34]. Usually, down-time can be extremely costly, and hence a system being able to tolerate a failure of one or more components while maintaining operation is extremely appealing. Of course, while the fault-tolerance comes at a price, there are techniques to quantify the increased reliability of the system, via reliability modeling. Such techniques involve a large number of mathematical equations and accurate data on component failure rates. Another metric that can be analyzed is Performability with its various forms: Steady State, Transient and Cumulative Performability (SSP, TP and CP respectively) and typically relates failure-rates to rewards at different system states [35, 36]. This will become clearer in the coming sections.

The work presented focuses on network traffic simulation, system performance enhancement, fault-tolerance and performability. Simulations are conducted on OPNET Network Modeler and all results are subjected to a 95% confidence analysis [36, 37]. The remainder of this thesis is split into two main sections: NCS in Intelligent Transportation Systems (ITS) and Wireless NCS (WNCS) for Industrial Automation. The background and previous work of both applications shall be presented next.

2.3. BACKGROUND ON NCS FOR INTELLIGENT TRANSPORTATION SYSTEMS

Intelligent Transportation Systems (ITS) are one of the largest applications of NCS. From the automotive industry, to aviation and railways, NCS technology has enabled different systems on-board to communicate together and share the available communication networks, rather than have a completely independent network for every system [38–40]. With regards to the railway industry, there are several existing solutions available in the literature (LonWorks and Train Communication Networks are examples of such systems) [8, 9, 39–48]. A NCS on-board of a train can manage navigation, speed control, braking, safety, supervision, door operation, ventilation and lighting. Such critical elements of a railway system necessitate high sampling rates and no over-delayed or dropped packets. As technology matured, Ethernet was proposed as the main communication structure for the NCS on-board, in several studies [49–53].

2.4. PREVIOUS WORK ON NCS FOR ITS

With the increasing luxury in different forms of transportation, passengers on airplanes, buses and trains now have internet access (wired/wireless) and even interactive video screens. This 'entertainment' load also requires a network infrastructure and a sharing of this infrastructure between control and entertainment data is proposed in [50–53]. The system presented in [50], debuted the idea of sharing a Gigabit Ethernet (GbE) network between the control and entertainment loads on-board of a train-wagon. The SAs all operated using the same sampling period, communicating with a dedicated controller/control server (K), either with a sampling period of 1ms or 16ms, based on the IEC 61375 standard [44]. The study concluded that the use of GbE for both a control and entertainment load would be a suitable solution on-board of a train network, guaranteeing correct packet transmission/reception with delays within sampling rate constraints.

In [51], the system presented in [50] was revisited to integrate fault-tolerance at the controller level. The control and entertainment servers were allowed to take over for the other in the event of a failure. The entertainment load in the event of a failure

would be sacrificed and the remaining machine would be in charge of control data only. This study showed the true advantage of a shared NCS between the control and entertainment loads, proving the system could tolerate the failure of one of its machines, while maintaining correct operation.

Finally, in [53], fault-tolerance of a different form was introduced. Triple Modular Redundancy (TMR) was employed at the sensor level, whereby every sensor is replaced with three redundant but active sensors, and by majority vote, a decision is made. This technique allows the failure of up to one sensor and the system would not experience any errors.

In the next section, the background for the application of Wireless NCS (WNCS) in Industrial Automation will be presented.

2.5. BACKGROUND ON WNCS FOR INDUSTRIAL AUTOMATION

Industrial Automation is another application of NCS that is also a major driving force in the innovation of NCS. Sensors and actuators are a fundamental component in any automation system. Ethernet in industrial automation has also been extensively supported in research [2, 14–17, 30–33]. Fault-tolerance is also a critical aspect of industrial automation, because in many cases, production lines run 24 hours a day, 365 days a year, except for down-time due to preventive or standard maintenance, cleaning or system upgrades. A fault in the production line, causing degraded performance or even an hour of down-time can incur significant financial losses.

2.5.1. WIRELESS INTERFACE FOR SENSORS AND ACTUATORS (WISA) BY ABB

Apart from the determinism favored in the past as described in Sec. 2.1, NCSs have depended solely on wired connections. While stability, reliability and noise tolerance were guaranteed using wired methods, cables are costly and require intensive maintenance and organization. Cables also hinder mobility and are under threat of being cut or severed due to the hazardous attributes of a typical factory-floor environment. The introduction of wireless protocols for intercommunication between nodes means reduced costs, increased mobility and simplicity of installation and

maintenance. There are many studies regarding Wireless NCS (WNCS) available in the literature [54–60]. One of the most robust and innovative WNCS solutions available is Wireless Interface for Sensors and Actuators (WISA) designed and produced by ABB [54–56]. WISA compares between WiFi, ZigBee and Bluetooth with regards to data rate, power consumption and coverage and chooses to use a customized nonstandard version of Bluetooth [54–56, 61–63] that serves as the communication protocol between sensor, actuator and controller modules. The system also offers a unique method of wireless powering for its nodes, using magnetic coils [54–56]. A typical workcell can be seen in Fig. 1 [64].

A workcell is around 3×3m, containing up to 120 1-bit nodes [54–56]. Table 1 shows some of the system attributes and shall be referred to in due course, further system parameters can be found in [54–56]. The lack of a standardized protocol however, is quite a set-back for the system.

Figure 1. WISA Workcell Example [56]
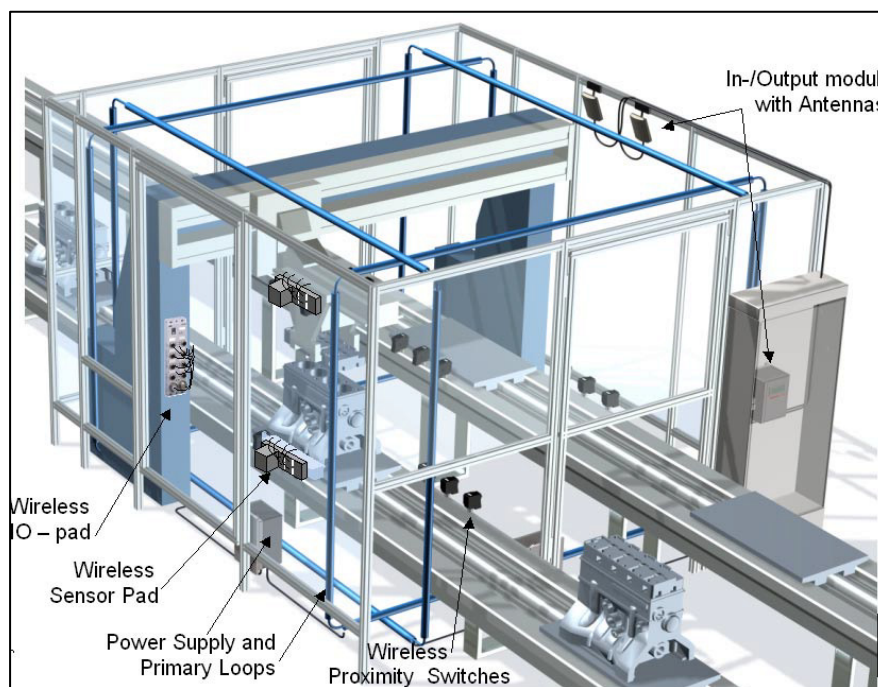
Table 1 – WISA System Parameters [56]

Maximum number of nodes to one base station/Cell ID	120
Maximum latency from WISA air interface	20ms
Minimum distance to non-interfering WLAN/Bluetooth	25/16 m
Maximum number of WLANS within interfering distance	1
Maximum output RF power	1 mw

2.5.2. NOISE/INTERFERENCE IMMUNITY

The main threat to a WNCS (making wired NCS solutions more appealing) is the effect of noise/interference on a factory-floor due to heat, welding and/or mechanical vibrations, among other sources [54–56]. An exhaustive experiment was conducted in [54–56] concerning a range of factory-floor forms of noise/interference (e.g. arc/spot welding). The result of these experiments showed (using a spectrum analyzer) that even uncommon and unpredictable forms of interference/noise (such as that from arc/spot welding) will saturate at around 1.8GHz [54–56]. Hence, the WISA system was deemed 'immune' to noise/interference from sources of such on the factory-floor. The conclusion drawn from these experiments can be stated as follows: A WNCS with an operating frequency in the Industrial, Scientific and Medical (ISM) band need only be concerned with sources of noise/interference that will attach the ISM band. Other experimental methods for analyzing the effects of noise are presented in [60].

2.6.   WiFi WNCS – PREVIOUS WORK

2.6.1. SINGLE-CELL MODEL

A WNCS that utilizes standardized, off-the-shelf equipment is currently unavailable in the market and is a very appealing concept due to simplicity of integration, compatibility and cost-efficiency. In [65], such a system, utilizing strictly IEEE 802.11b and Switched Ethernet is proposed and investigated, using WISA performance metrics as a benchmark. The model proposed is built as shown in Fig. 2.

This model as shown is a uniform square workcell with side length 3m. The workcell itself contains a total of 30 sensors (S), 30 actuators (A) and two WiFi access points (BSS1 and BSS2). Each access point is assigned to 50% of the SAs (as shown in the figure) and utilizes non-interfering WiFi channels. With a data rate of 11Mbps, the access points operate at a transmit power of 1mW (the minimum WiFi power, for maximum power conservation), identical to the WISA system transmit power. Of course, the data rate is a step up versus WISA system and hence, the payload of the WiFi WNCS is chosen to be a 10B User Datagram Packet (UDP) with a sampling period of 40ms (allowing a 20ms delay per link as is specified by WISA, with 2 links in total). The decision to use UDP versus other protocols which require

acknowledgment packets and allow retransmissions is based upon the recommendations in [16].

Figure 2. Single-Cell Model [70]
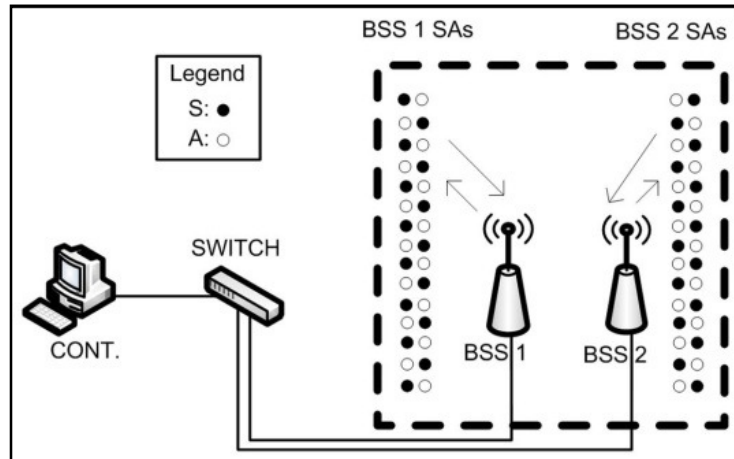
The study [16] suggested the advantage of UDP as the system can make full use of the available bandwidth by minimizing acknowledgments. This lack of acknowledgments can be considered a disadvantage for nodes using UDP because a transmitting node has no way of knowing whether its transmitted packet has been received by the destination or whether it was dropped. Hence, in all simulations, packet drops are not tolerated and such a criteria must also be guaranteed when implementing a physical system.

The access points are wired to an Ethernet switch placed outside the workcell, which is then wired to the controller. In a real production line, the controller does not necessarily have to be in a specific place with regards to the cell and hence is chosen to be placed outside the perimeter of the workcell.

As was concluded by the WISA experiments, an ISM band system as was proposed in the WiFi WNCS has no noise/interference sources to be concerned with in a factory-floor other than ISM band sources [65]. In a factory-floor environment, the number of ISM band sources external to a WiFi WNCS can be very limited. Unlike an office or a home environment, there are no personal WiFi networks, Bluetooth users etc. The most realistic case to investigate was chosen to be that of a service engineer(s) also operating on WiFi. Several different scenarios of a WiFi node(s), on the perimeter of the workcell, were modeled to represent a service

engineer(s) communicating via the workcell access points with the controller. This WiFi node(s) communicates using the same channel as the portion of the WNCS to be interfered with (in the case of two laptops, the entire system). The communication is in the form of an FTP file requested every 0.5 seconds. This FTP file size is gradually increased in order to find the maximum tolerable file size while maintaining correct performance (zero over-delayed or dropped packets). As the WISA system is the reference or benchmark, to which the WiFi system is being compared, all end-to-end delays and packet reception/transmission metrics must be maintained if not surpassed. The WISA system, as shown in Table 1, allowing retransmissions, guarantees maximum packet latency *per air link* of 20ms. The WiFi system [65] guarantees a maximum packet end-to-end delay *per link* of 16ms in the presence of noise with a 95% confidence analysis. It is important to note that there is a significant difference between the OPNET end-to-end delay and the air link specified in the WISA document. The end-to-end delay result given by OPNET simulates all layers from Application (transmitter) to Application (receiver) while the air link specified by WISA implies only the physical layer. The term link is defined as from a sensor to the controller, or from the controller to the actuator.

The use of WiFi and Ethernet in the system necessitates (by standard protocol) the use of Carrier Sense Multiple Access with Collision Detection/Avoidance (CSMA/CD and CSMA/CA). As expressed in Sec. 2.1, this introduces a source of non-determinism, due to the use of BEB and hence statistics collected must be subjected to a confidence analysis. All results presented in this thesis are based on a 95% confidence analysis.

2.6.2. CELL CONCATENATION

With the feasibility of a WiFi single cell investigated and published, the next logical step would be to expand. A production line is not composed of a single workcell and there is a need to concatenate several workcells along the line. It is important to insure that concatenating several cells of the same WiFi WNCS proposed in the previous section will not cause violations in meeting system requirements. As such, the effect of neighboring cells on one another must be studied. In [66], two cells built as in [65] are simulated on OPNET. Fig. 3 shows the layout used.

Due to the single-cell model proposed in [65] requiring two access points, and hence two non-interfering WiFi channels, when modeling a two cell system, the issue of co-channel interference arises. Now, there is a total of four access points, yet the 802.11b standard only offers three non-interfering channels (Ch1, Ch6 and Ch11) [61] and hence one of the three channels will have to be reused. The frequency reuse introduces the issue of co-channel interference and the effect of this co-channel interferer must be studied.

Figure 3. Two-Cell Model
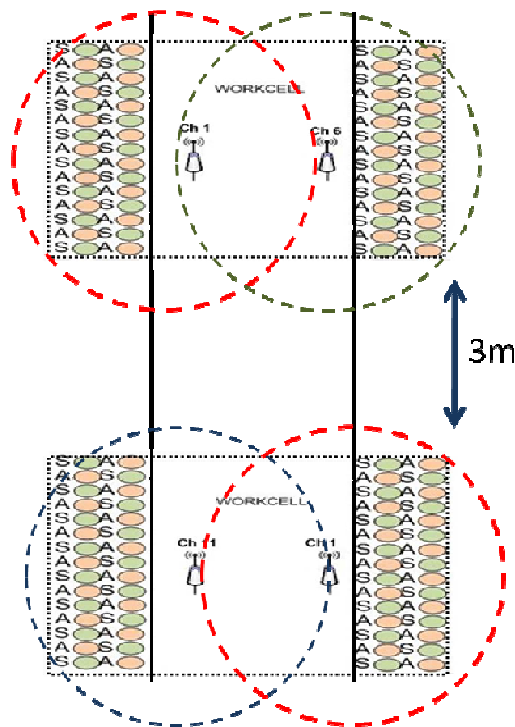
After conducting several experiments on OPNET Network Modeler, it was found that concatenation of two cells was impossible below a distance of 2m (inter-cell distance) using a maximum Packet Reception Power Threshold (PRPT) of -50dBm. The PRPT is directly analogous to Receiver (R_x) sensitivity but is an inversely defined parameter. PRPT is a value that indicates a signal strength, below which a packet is not recognized. The confusion comes only when saying increasing or decreasing PRPT. Note: Increasing PRPT implies a decrease in R_x sensitivity and vice versa. The reasons for such values were not studied mathematically; however this shall be further investigated in this thesis work. For safety reasons, a guard distance of

1m was added to the 2m inter-cell distance and all simulations using the topology presented in this section used a 3m inter-cell distance.

Interference was modeled on the non-reused channels, as the reused channel was deemed off-limits to nodes outside their workcell. Again, the system guaranteed zero packets dropped and all end-to-end delays per link (with a 95% confidence analysis) below 16ms.

2.6.3. WIRED FAULT-TOLERANCE AT THE CONTROLLER LEVEL

As was presented in Sec. 2.2, fault-tolerance is an important field of study and its applications in NCS are numerous. The advantage of fault-tolerance of any form in an industrial application is that of reducing downtime. Downtime on a factory-floor is a direct source of financial losses and is most undesired. Any technique employed that would guarantee correct performance (if not full performance) during the event of a failure is a worthy topic to investigate. This is the main focus of [67].

Controllers on the production line are now becoming more intelligent, more powerful and leaning towards Industrial Personal Computers (IPC) [68]. As such, a controller need not be capable of only one task/function; it can be capable, in the event of a neighboring controller's failure, to take over its neighboring workcell's tasks. In [67], the concatenated system modeled in [66] is revisited to integrate fault-tolerance at the controller level.

After investigating concatenation of several cells, it would be an advantage to utilize the neighboring controllers for fault-tolerance in the event that either failed. The two cells are *wired* (also using 1GbE) together and some modifications are made to enable fault-tolerance. All sensors send a copy of each sample to both controllers, so that each controller has the most up-to-date data. Each controller also sends a watchdog packet to its neighbor, alerting the neighbor of its status. This packet is exchanged every half of a control sampling period (every 20ms) to increase reliability and in the event of a controller failure, the neighbor would be aware of the failure and take corrective action. Fig. 4 shows a simplified representation of the communication occurring in both the fault-free and fault-tolerant scenario.

The system was simulated in both the fault-free and faulty state, with the same noise philosophy introduced in the previous section, as in [66]. Conclusions of the

study showed that the system could tolerate the failure of either controller and continue correct operation with zero dropped packets and all delays per link within a 16ms benchmark (after a 95% confidence analysis).

Figure 4. Fault-Tolerance Overview: Fault-Free (left), Faulty (right)
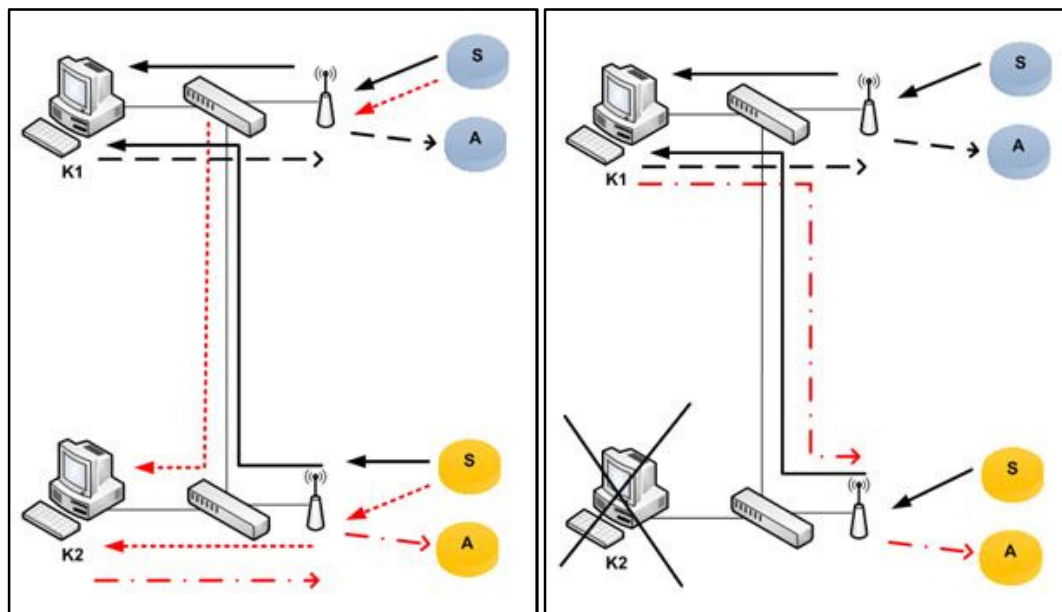
2.6.4. PREVIOUS WORK SUMMARY

A WNCS utilizing strictly standard IEEE 802.11 and 802.3 without modifications was proposed and studied in several stages, exceeding performance metrics specified by the existing solution: WISA by ABB. A single-cell model was designed and simulated on OPNET, to be further investigated for concatenation of several cells and fault-tolerance at the controller level. The resulting publications are [65–67].

2.7. PROBLEM STATEMENT

2.7.1. NCS FOR INTELLIGENT TRANSPORTATION SYSTEMS

Previously, NCS on-board of train wagons were investigated incorporating fault-tolerance at the server level. However, there exists significant room for improvement as the modeled systems experience a high level of entertainment load degradation during failure. Also, the control load modeled does not include a mixture of different sensor/actuator sampling periods. These shortcomings shall be addressed in this thesis and further contributions shall be presented in Sec. 3.

2.7.2. WIRELESS NCS FOR INDUSTRIAL AUTOMATION

WNCS, being a relatively new field, and solutions presented in industry being non-standard, there is a need to further fine-tune and expand on previous work conducted during my undergraduate thesis: A WiFi WNCS. Fault-tolerance, concatenation and performability will be studied among other points in Sec. 4. It is critical to note that all work mentioned in this thesis is based on WiFi simulations using OPNET Network Modeler, which models a free space environment. This does not take fading and/or reflections into account, so all results presented are within a significant guard band in delays. In a hardware implementation, this guard band will facilitate delay increase while satisfying system requirements.

3. NCS FOR INTELLIGENT TRANSPORTATION SYSTEMS

3.1. PROPOSED TRAIN-WAGON MODEL

3.1.1. NETWORK ARCHITECTURE

The model proposed in this section (shown in Fig. 5) describes the basic unit to be studied throughout the remainder of Sec. 3 [69]. This model, while similar to the models presented in [50–53], contains several fundamental differences: the grouping of sensors and actuators and the modeling of different sampling periods within the same system among further enhancements to be discussed later on.

Figure 5. Train-Wagon Architecture
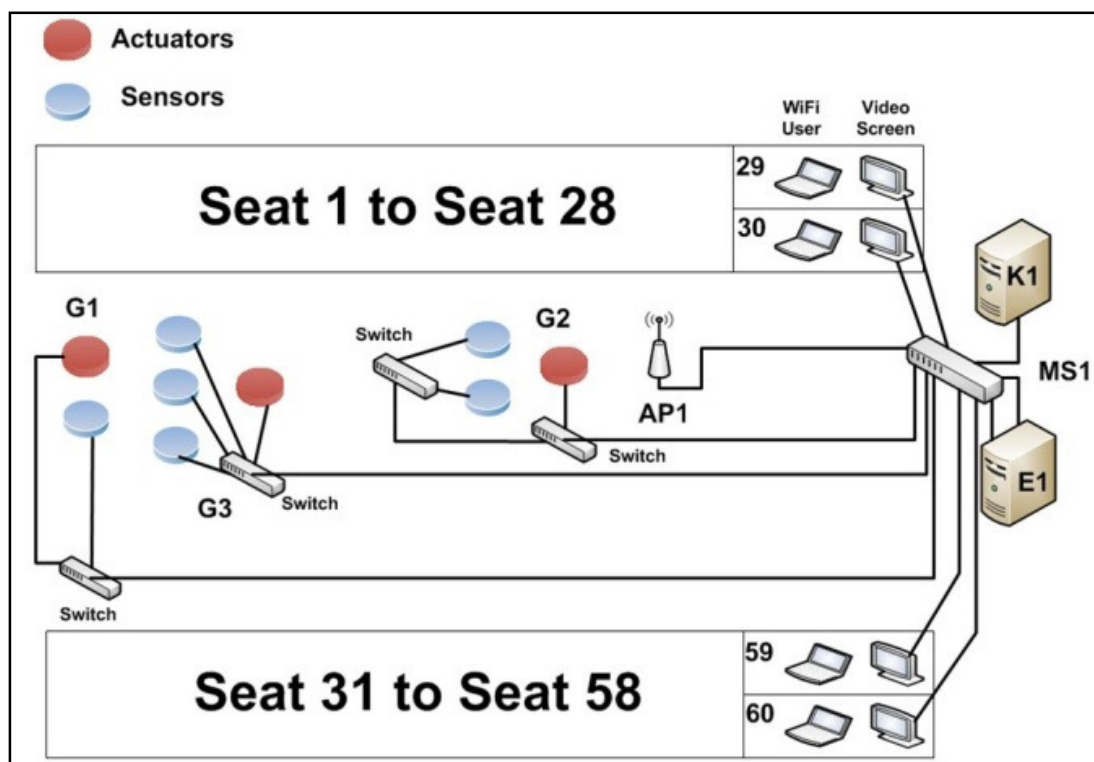
Based on the IEC 61375 standard, a typical train-wagon NCS would contain a very large number of sensors and actuators using different sampling periods, to serve different applications with different levels of criticality [44]. The number of sensors and actuators was selected to be 250 nodes in total, based on the IEC standard [44]. These nodes are split into several groups. Group 1 (G1), Group 2 (G2) and Group 3

(G3) can be described accordingly: G1 is 30 sensors and 30 actuators, where every actuator, has one corresponding sensor, operating with a 1ms sampling period. G2 contains 100 sensors to 50 actuators (2:1 ratio) using a 16ms sampling period and G3 contains 30 sensors to 10 actuators (3:1) using a 16ms sampling period. The controller/control server (K) is connected to all sensors and actuators via a 1GbE network, using the minimal number of switches, by using standard switches with 128 ports each and a forwarding rate of 6.6Mpps (the default OPNET model value). The proposed forwarding rate is far less than many available components and yet it shall be used as is [36]. The nodes are all placed generically in a simplified layout, to maximize distance from the K, while in a realistic scenario the sensors and actuators would be more evenly distributed. The selected positions increase propagation delay to model the worst-case scenario.

In a train-wagon at this time, 60 seats, split into pairs along the sides of the wagon is a common setup [69]. Each seat has been modeled, having a video screen, streaming DVD quality video and in the worst case scenario, a passenger accessing the WiFi network (served by the WiFi AP in the center of the wagon) with multiple simultaneous applications [61]. Each passenger is performing four of the standard *heavy* applications available on OPNET Network Modeler: Sending/receiving emails, database access, web browsing and a file transfer protocol application (FTP). After some initial simulations, the previously described WiFi load was found to require a maximum of 6Mbps bandwidth, offered by the entertainment server, connected via the GbE network. As this network is shared with the control load, the maximum bandwidth offered to the WiFi users must be limited to this value, to ensure that this load does not interfere with the control load. The DVD quality screens are wired to the GbE network and are modeled in terms of streams, rather than screens. This requires some clarification. The passengers in total are 60, each with their own screen. Each user could be watching a completely different stream or they could all be watching the same stream. Hence, for the sake of modeling the worst case scenario, every screen present in the model, represents a different stream. Next, the initial fault-tolerance philosophy shall be introduced.

3.1.2. FAULT-TOLERANCE

Two identical wagons, each as described above are cascaded, as would be done on a train. The main switches of each wagon are interconnected. This model can be seen in Fig. 6.

Figure 6. Two-Wagon Model [54]
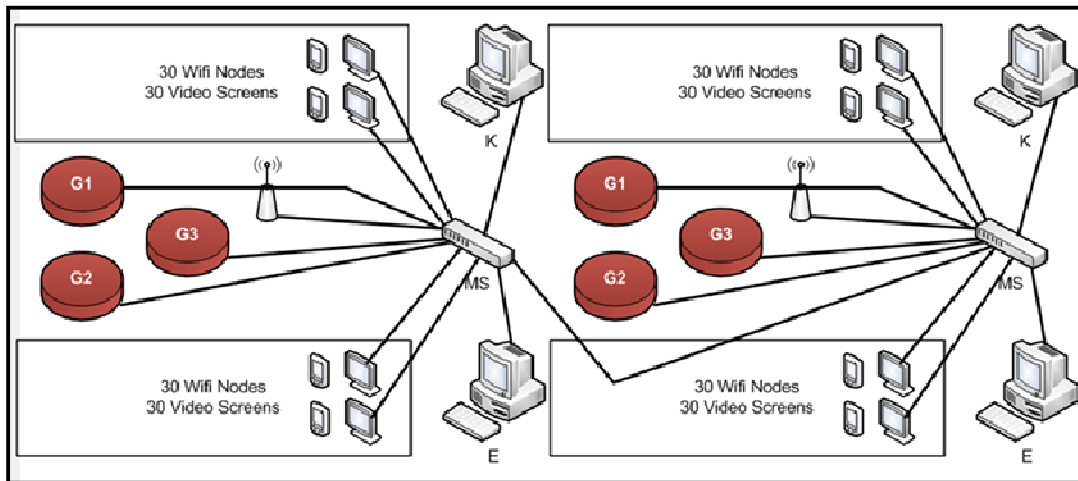
There is now a total of 120 video streams and 120 WiFi users, 500 SAs, two controllers/control servers (K_1 and K_2), and two entertainment servers (E_1 and E_2). These servers, being susceptible to failure, are targeted for fault-tolerance in this study. Each server must be able to take over for another in the event of a failure of one or more machines. For this to be possible, each of the servers exchanges a watchdog signal with its fault-tolerant counterparts. This signal represents an awareness of the status of each of the machines. If a server fails, it would stop sending its "I'm alive" signal, and the remaining controllers would become aware of its failure, in order to take action.

In order for the transition between machines to occur smoothly with minimal data loss, all machines must have the most recent samples (sent by sensors) as they are generated. To accomplish this, every sensor is made to send an identical copy of each sample, to every operational server, so in the fault-free case, for example, each sensor would send four copies of its data, directed at K_1, K_2, E_1, and E_2. While the sending of multiple copies of each sample increases the load on the network, it facilitates fault-tolerance, thereby increasing reliability.

17

3.1.3. SCENARIOS STUDIED

The previously described system was built and studied on OPNET Network Modeler in two main stages: single wagon and two wagons. For both scenarios, the fault-free case was modeled, followed by the worst-case scenario, where all but one server remained. In the single wagon model, the full control load and entertainment load are handled by their respective servers in the fault-free scenario. Next, one of the machines is failed, and the remaining server handles the full control load and as much entertainment load as possible, without causing violations in the control load.

The second stage involves two identical wagons as shown in Fig. 6. Again, the fault-free scenario is modeled first. Next, the worst-case scenario is modeled, where three out of the four available servers have failed, and again, the entire control load is carried by the remaining machine, with as much entertainment load as possible while maintaining correct control operation.

The following list shows the details of the OPNET models used [36]:

1. Sensors, Actuators, Servers, Screens: Ethernet Workstation Advanced

2. WiFi nodes: WLAN Workstation Advanced

3. WiFi Access Point: WLAN Ethernet Router Advanced

4. Switches: 128 Port Ethernet Switch Advanced

5. Cables: 1GbE

3.1.4. RESULTS

After the previously described cases were simulated different metrics were analyzed. The main metric used to measure system performance is the number of dropped packets and the end-to-end delay. The end-to-end delay measured by OPNET Network Modeler is defined as the time taken from when a packet is transmitted to when it is received by the destination. This delay includes and models all layers of the network model, containing all forms of processing, queuing, encapsulation,

decapsulation and propagation delays [36]. In this system, the delay from sensor to controller, and from controller to actuator, are added, to give the total delay taken for a sample to be sent by the sensor until the control word is successfully received by the actuator.

Each simulation is run with 33 seeds, for statistical analysis (see Appendix) and the maximum total delay experienced in all runs is obtained. The following figures (Figs. 7 to 10) present several OPNET Network Modeler end-to-end delay screenshots. In each of these figures, the x-axis is the simulation time in minutes and seconds, and the y-axis shows the packet end-to-end delay in seconds. Note, this is not the full duration of the simulation, only a small interval.

Figure 7. Two-Wagon Fault-Free G1 (K to A) [69]
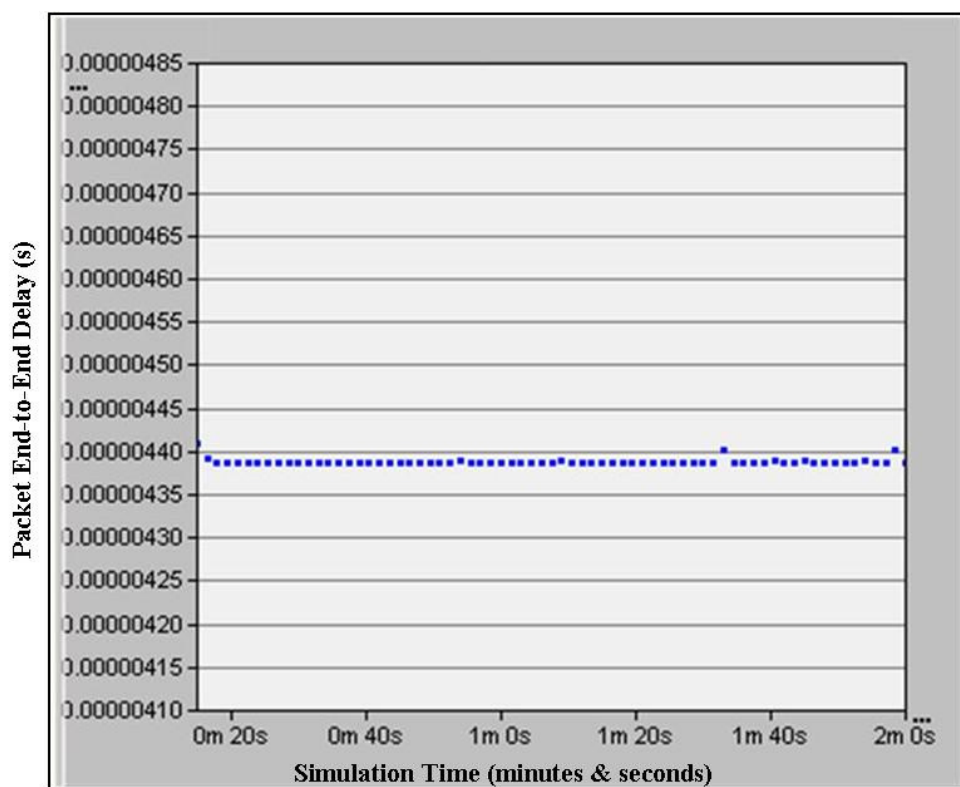
Figure 8. Two-Wagon Faulty, G1 (K to A) [69]
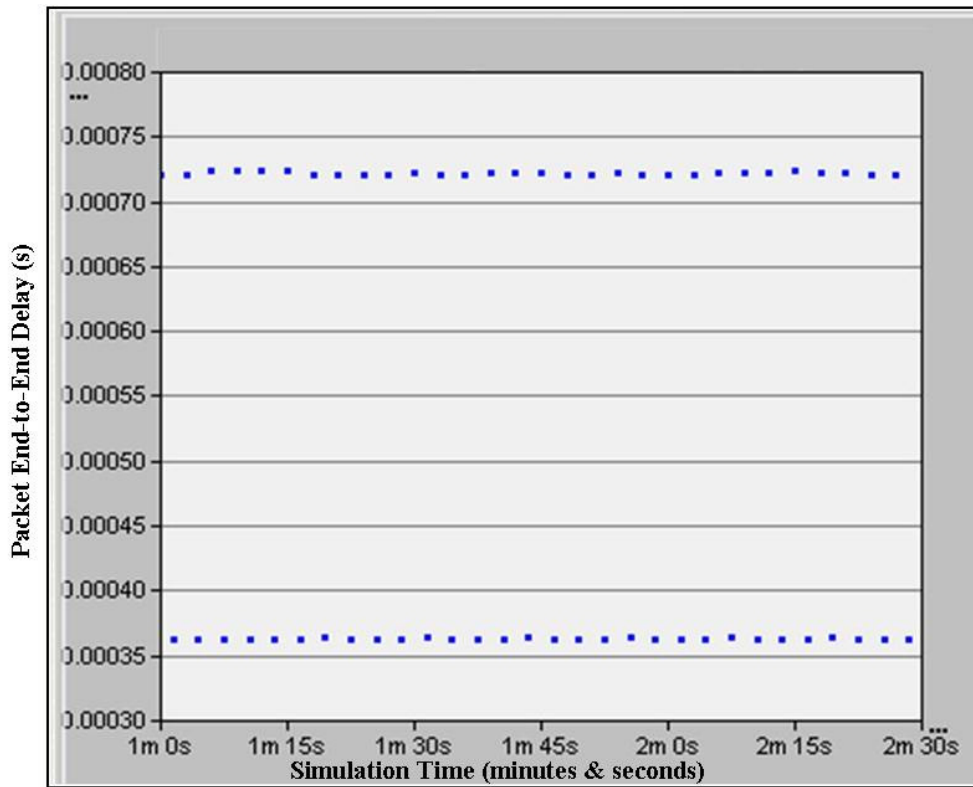
Figure 9. Two-Wagon Faulty, G2 (K to A) [69]
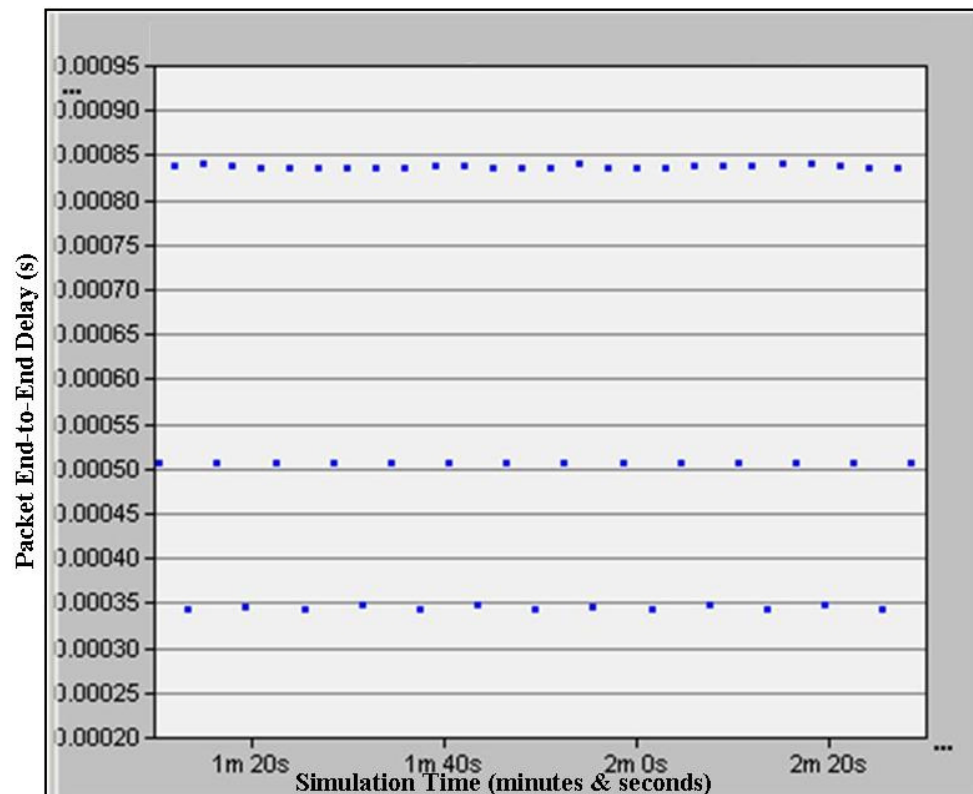
Figure 10. Two-Wagon Faulty, G3 (K to A) [69]
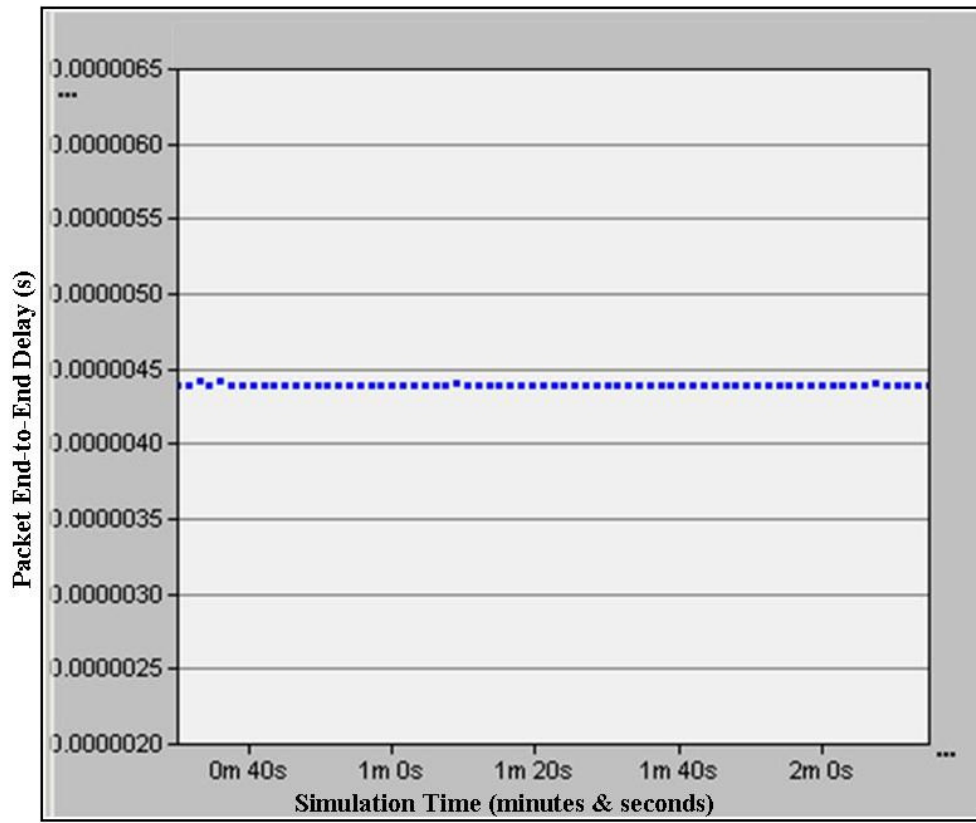
Table 2 shows the results of for the four previously described scenarios. The table columns represent: The number of wagons modeled (one or two), the number of operating servers (fault-free: 2 and 4, faulty: 1), the *maximum* total delay from a G1 sensor to a server, then to a corresponding actuator, the same for G2, and G3, the number of pulled Video Streams and the number of WiFi users.

Table 2 – Results Summary [69]

Wagons	Functional Servers.	G1 Delay (ms)	G2 Delay (ms)	G3 Delay (ms)	No. Video Streams	WiFi Users
1	2	0.010	0.011	0.011	60	60
1	1	0.751	0.870	0.876	6	60
2	4	0.016	0.013	0.026	120	60
2	1	0.772	0.908	0.922	6	60

The key take away from this table is the maximum delay experienced by any group. The entire control system is observed to experience an absolute maximum delay of 0.922ms. The ceiling for each group (G1, G2, and G3) is the corresponding sampling period. This means that G1, experiencing a maximum delay of 0.722ms, is

within the deadline of 1ms, and G2/G3 both experience a maximum delay of 0.922ms with a deadline of 16ms. These delays are resulting from 33 runs.

Another take away from the previous table is that the number of WiFi nodes is unchanging and the main degradation in entertainment load (depending on system state) is in the Video Streams. There are several points to note. Firstly, the reason for this degradation is that the WiFi load is not comparable (in terms of traffic size) to the Video Streams or the control load, and hence, a bounded 6Mbps WiFi connection, does not affect the control load. Secondly, it is critical to note that the number of active screens, or in other words, the number of passengers with an operational video screen, does not decrease. The degradation in the entertainment load is but a decrease in the maximum number of different, simultaneously playing streams. For the sake of simulation, each of these streams is modeled as a single screen, for two screens pulling the same stream would only create the load of one single stream.

3.1.5. INITIAL CONCLUSIONS

A single-wagon and two-wagon model, built using OPNET Network Modeler, with an Ethernet backbone, shared between the control and entertainment load. The entertainment load is composed of a WiFi user in every passenger seat as well as a DVD quality video stream displayed on the seat screen. The system incorporates fault-tolerance at the server level and the system is shown to tolerate the failure of up to one server, in the single-wagon model and up to three servers, in the two-wagon model. In both the fault-free and the faulty scenarios, the end-to-end delays experienced by a packet from sensor to controller, to actuator were always below the sampling rates of the control nodes. The control packets also experienced no packet drops and these results are all based on 33 simulation runs. In the worst-case scenario, where only one controller remains operational and all others have failed, both in the single-wagon or the two-wagon models, the control loads are unaffected, the WiFi load is unaffected, yet the maximum number of simultaneously playing video streams drops from 60 (or 120 in two wagons) to a total of six. This is a large drop and accordingly, the next section shall further investigate the single-wagon model in order to decrease the effect of a controller failure as well as analyzing the performability of the system.

3.2. SINGLE-WAGON ENHANCEMENT AND PERFORMABILITY ANALYSIS

3.2.1. ARCHITECTURAL ENHANCEMENTS

The basic, fault-tolerant, single-wagon model presented in Sec. 3.1 is further investigated in this section of the study in order to find the source of the extent of the degraded performance experienced in the scenario where one of the two servers has failed. Upon finding the source of this degradation, further experiments are conducted to find a way to reduce this degradation. The results of the previous section for the fault-free and faulty, unmodified architecture were revisited. Then, the faulty scenario, of one of two servers failed, while the remaining machine handled the full control and WiFi load, and as many DVD streams as possible (six out of 60), was re-simulated after several enhancement attempts.

There can be several reasons for a drop in the maximum tolerable number of DVD streams in the faulty scenario and in order to localize the issue, one must study the exact changes that occur upon transition from the fault-free scenario to the faulty scenario. Firstly, in the fault-free scenario, the control load has a full 1GbE cable, between the main switch and the control server, and the entertainment load has another, dedicated 1GbE cable between the switch and the entertainment server. Each load has its own dedicated switch Ethernet port as well as its own dedicated processor. When either of the servers fails, the system experiences a bottleneck in one, two or all three of the previously stated points. The faulty scenario has the control and (as much) entertainment load sharing a single switch Ethernet port, a single 1GbE cable and a single processor. Each of these three areas must be studied individually and in combination [70].

Prior to modifying the architecture in any way, the details of the unmodified system must be analyzed and compared with available components in the market. Firstly, the switch port, or more relevantly, its forwarding rate (at a default OPNET value) was set at 6.6Mpps (million packets per second). The Cisco Catalyst 3560, a high-end switch available in the market, has a much higher forwarding rate of 38.2Mpps [71]. Also available in the market at this time, are high speed cables, up to 100GbE [72]. To decrease costs for such enhancements, 10GbE cables are chosen as

the upgrades for the 1GbE cables linking the switch to each server [69]. Finally, the standard OPNET model used to simulate the servers must be compared to current available machines. The default OPNET processor type is a single-core, 0.333GHz CPU, Sun Ultra 10. Up to many years ago, this would be considered an obsolete machine, with current multiple core technologies, higher processing frequencies, parallel processing… etc. However, initial simulations showed that increasing processing power made no significant impact on the maximum supported entertainment load during the faulty scenario, indicating that the more critical bottlenecks to be addressed are the cables and switch forwarding rates.

This gives a total of four scenarios to compare:

1. Unmodified: (1GbE – 6.6Mpps)
2. Switch: (1GbE – 38.2Mpps)
3. Cable: (10GbE – 6.6Mpps)
4. Hybrid: (10GbE – 38.2Mpps)

Each scenario was simulated on OPNET, again, with 33 runs. All previously mentioned control load benchmarks (delays and packet loss) were met and the maximum supportable entertainment load was found. A sample of the end-to-end delay results (from scenario 4) can be seen in Figs. 11 and 12 (x-axis is simulation time in minutes and seconds, y-axis is delay in seconds). Note that all delays are below the required benchmarks (1ms for G1 or 16ms for a G2/G3). The low-valued points in Fig. 12 are indicative of very low delays and not dropped packets. Table 3 shows a summary of the maximum number of DVD Video streams for each architectural scenario. Each scenario has the full WiFi load supported and a control load that is operating with zero packet-loss (no dropped packets) and all packets arriving within system deadlines.

Figure 11. Single-Wagon Faulty (S to K) [70]
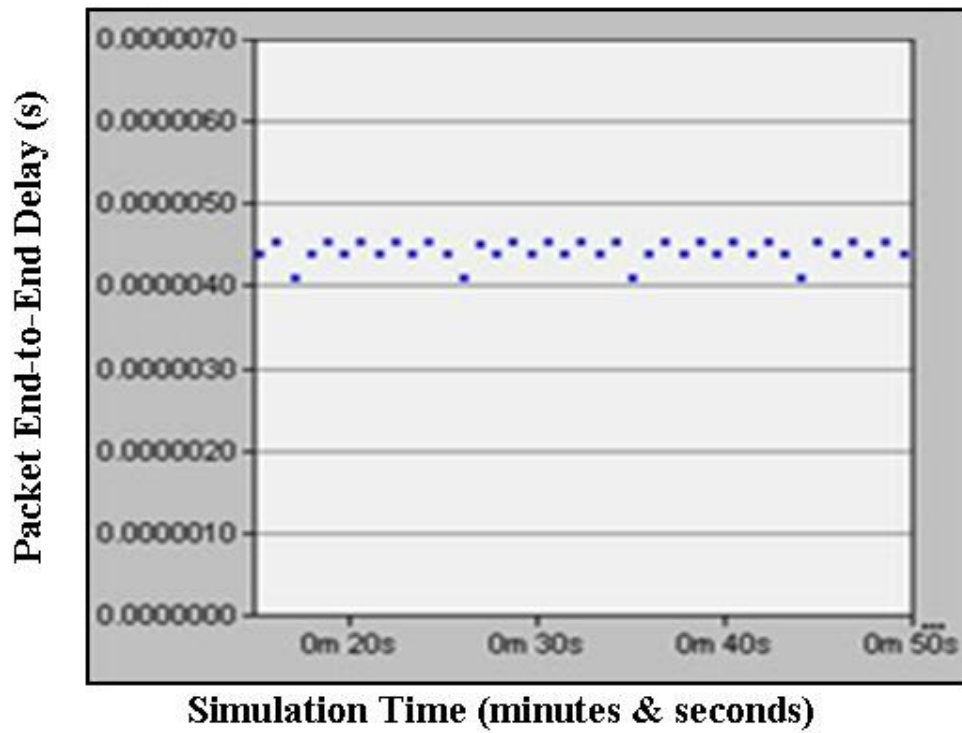
Figure 12. Single-Wagon Faulty G1 (K to A) [70]
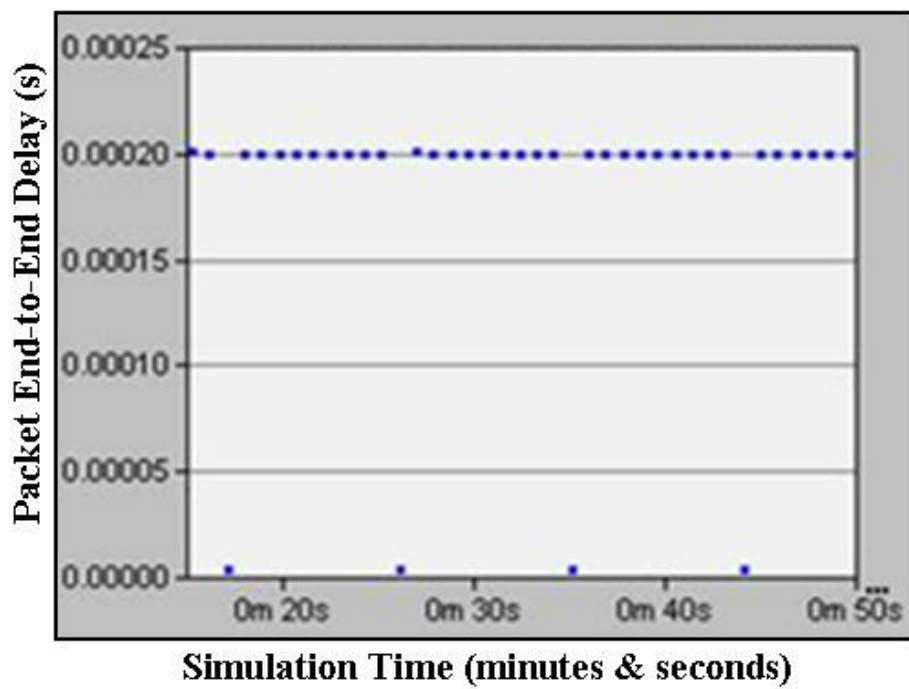
Table 3 – Maximum Entertainment Load for Each Scenario [70]

Scenario	Operational Server(s)	MS Forwarding Rate (Mpps)	Cable (GbE)	No. of DVD Streams
Fault-free	2	6.6	1	60
1	1	6.6	1	6
2	1	38.2	1	7
3	1	6.6	10	34
4	1	38.2	10	52

Scenario 4 was found to be the one that experienced the least delays, with a maximum total delay from any sensor to any actuator (both in fault-free and faulty scenarios) of 0.6946ms. This hybrid scenario (scenario 4), using both an upgraded cable and a higher switch forwarding rate was found to also offer the minimal degradation in entertainment load: supporting the full WiFi load as well as 52 streams, 86.7% of the full fault-free load (60 streams).

3.2.2. PERFORMABILITY ANALYSIS

The system proposed in the previous section guaranteed complete and correct operation of the control part of the NCS both in the fault-free and faulty scenarios. There is however, a change in the entertainment load offered, depending on the system state and this motivates the following part of the study: developing a performability analysis. The main purpose of the performability analysis is to relate failure data with reward, depending on the system state. In order to define reward, one must first analyze the services the system offers: The control function, the WiFi load and the video streams. In a production line system for example, reward can be defined as the yield of the system, depending on its state. If the production line output drops from 100 units/hour (100%) in the fault-free state and 70 units/hour (70% during a failure state); the yield would be used as the value representing reward. In the proposed system, the control load and the WiFi load are both unchanging and hence the reward would be the maximum number of supported video streams depending on the state.

The developed performability model can also be used to quantitatively compare the different enhancement scenarios proposed in the previous section. In effect, the Transient Performability (TP) to be studied, will give a metric relating both reliability

and performance simultaneously [34, 35]. In order to calculate TP(t), a Continuous Time Markov Chain is presented in Fig. 13 to model the reliability of the proposed system.

Figure 13. Single-Wagon CTMC [56]
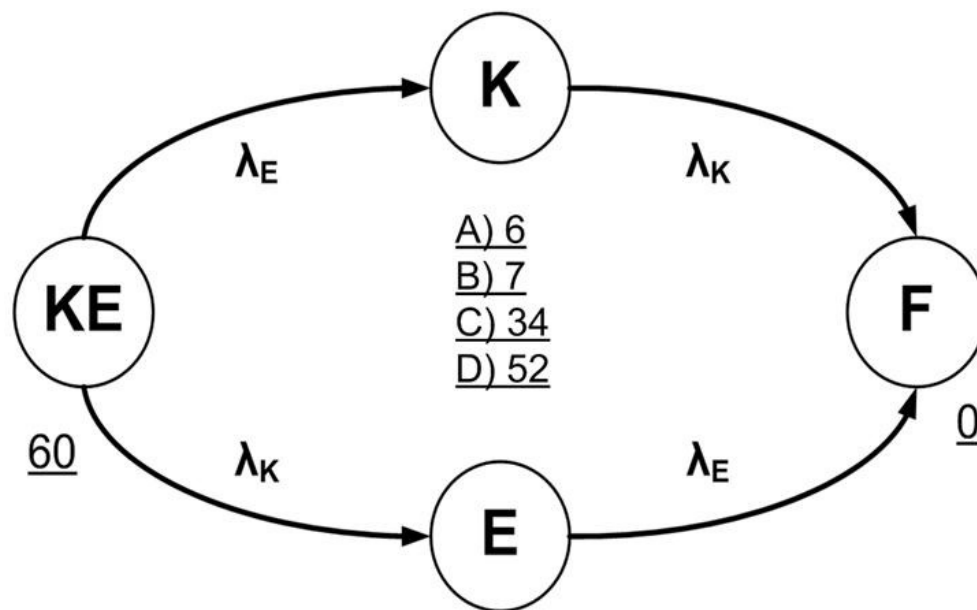
Each of the states of the CTMC has a number corresponding to the reward for each of the *four* modeled scenarios (presented in the previous section). In states K and E, the reward depends on the architecture modeled: Scenario A) represents the unmodified architecture, B) the upgraded switch, C) the upgraded Cable and D) both upgraded switch and cable. In state KE and F, the reward is not dependant on the architecture. In this CTMC, repair rates are not included because it is assumed that no maintenance is conducted during the trip.

The first state, KE, is the initial state, where the system is in the fully operational mode. Depending on which server fails first, the system will move to either state K (if E fails first) or state E (if K fails first). The transitions are labeled λ_K or λ_E, depending on which has failed, where λ_K is the failure rate of the control server and λ_E is the failure rate of the entertainment server. While at the second level (being at state K or E), another failure would send the system to the total failure state (state F).

Now, the probability of being at any of the states at time t is $P_i(t)$, where $i \in$ [KE, E, K, F]. Using the following Chapman-Kolmogorov (CK) equations, the transient probability can be obtained [34].

$$\frac{d\mathbf{P}}{dt} = \mathbf{P} \times \mathbf{T} \qquad (1)$$

$$\mathbf{P} = (P_{KE} \quad P_E \quad P_K \quad P_F) \qquad (2)$$

$$\mathbf{T} = \begin{pmatrix} -(\lambda_K + \lambda_E) & \lambda_K & \lambda_E & 0 \\ 0 & -\lambda_E & 0 & \lambda_E \\ 0 & 0 & -\lambda_K & \lambda_K \\ 0 & 0 & 0 & 0 \end{pmatrix} \qquad (3)$$

It can be assumed that at time $t = 0$, the probability of being in any state other than KE is 0. Hence, $P_{KE}(0) = 1$ and $P_K(0) = P_E(0) = P_F(0) = 0$. Using this initial assumption one can solve the CK equations in closed form as shown next:

$$P_{KE}(t) = e^{-(\lambda_E + \lambda_K)t} \qquad (4)$$

$$P_E(t) = \left(e^{-\lambda_E t}\right)\left(1 - e^{-\lambda_K t}\right) \qquad (5)$$

$$P_K(t) = \left(e^{-\lambda_K t}\right)\left(1 - e^{-\lambda_E t}\right) \qquad (6)$$

$$P_{KE}(t) + P_K(t) + P_E(t) + P_F(t) = 1 \qquad (7)$$

$$TP(t) = \sum_{i \in S} P_i R_i \qquad (8)$$

where:

S is the set [KE, E, K, F]

R_i is the reward at state i (depending on the proposed architecture)

The reward to be used in the equation can be obtained (as previously described) from Table 3 or from the CTMC showing the maximum number of supported video streams depending on the architecture to be analyzed for performability. The measure of performability can also be used to analyze the cost-effectiveness of the system. As was stated in Sec. 2.2, fault-tolerance comes at a price and it is often necessary to quantify the return that one would get for investing in a (more) fault-tolerant system. Here, performability will be used to show the enhancement to the system when a more reliable server is purchased (i.e. with a lower λ_K or λ_E. The following analysis is conducted in several stages:

1. Comparing $TP(t)$ for scenario 4 using different failure rates: λ_K = 1, 0.5 and 0.25 failures/week.

To give an example of the benefit of such a study, it can be shown that when comparing a machine of λ_K=1, 0.5 and 0.25 failures/week, after four weeks of operation, the transient performability for a λ_K of 0.25 increases by 946.8% compared to a lower-end machine with a lower reliability (a higher failure rate λ_K=1). This increase justifies the more investment in a more costly but more reliable machine to serve as control/entertainment server. Fig. 14 shows $TP(t)$ for different values of λ_K and it can be observed that a higher-end machine (lower failure rate) will result in a higher performability.

Figure 14. Transient Performability for Different Failure-Rates [56]
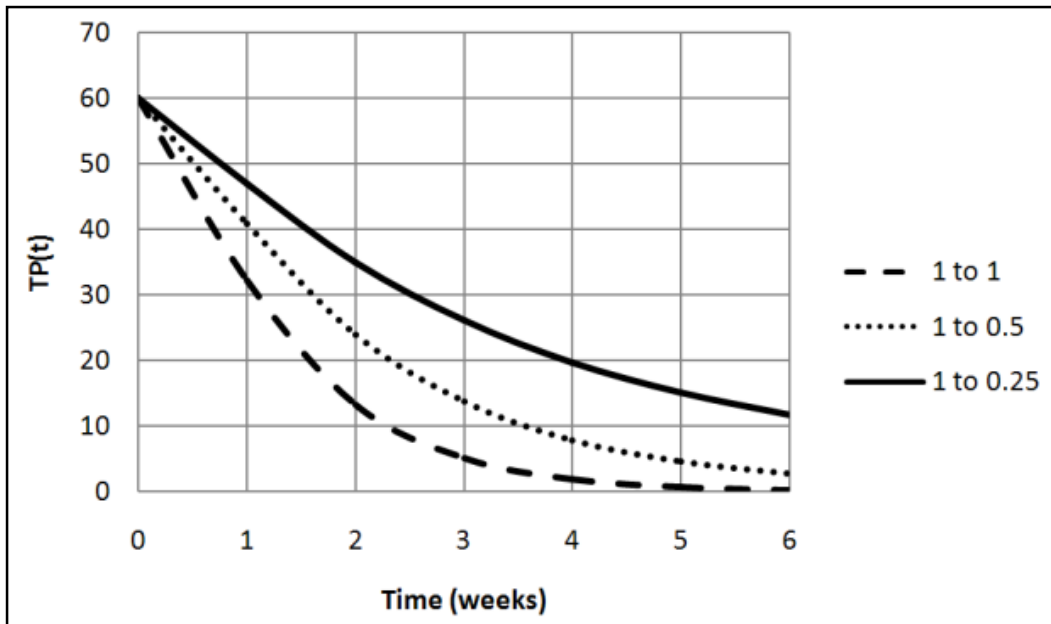
2. Comparing Scenarios 3 and 4 (stated in Table 3) with λ_K = 1 failure/week

The take away from this comparison, is to quantitatively represent the difference between enhancements on the system, again to justify a more costly investment (for higher-end equipment). To present some numerical values, when comparing Scenario 3 to Scenario 4, investing in a 10GbE as well as a switch with a higher forwarding rate (38.2Mpps) rather than just a cable upgrade and using the standard switch, results in a $TP(t)$ (at 2 weeks) that is 13.27 rather than 9.05 (46.5% increase due to a more

costly switch). The comparison of the different architectures can be seen in Fig. 15. The dashed line represents Scenario 3 (switch of 6.6Mpps forwarding rate) and the solid line Scenario 4 (switch of 38.2Mpps forwarding rate).

Figure 15. Transient Performability for Different Architectures [56]
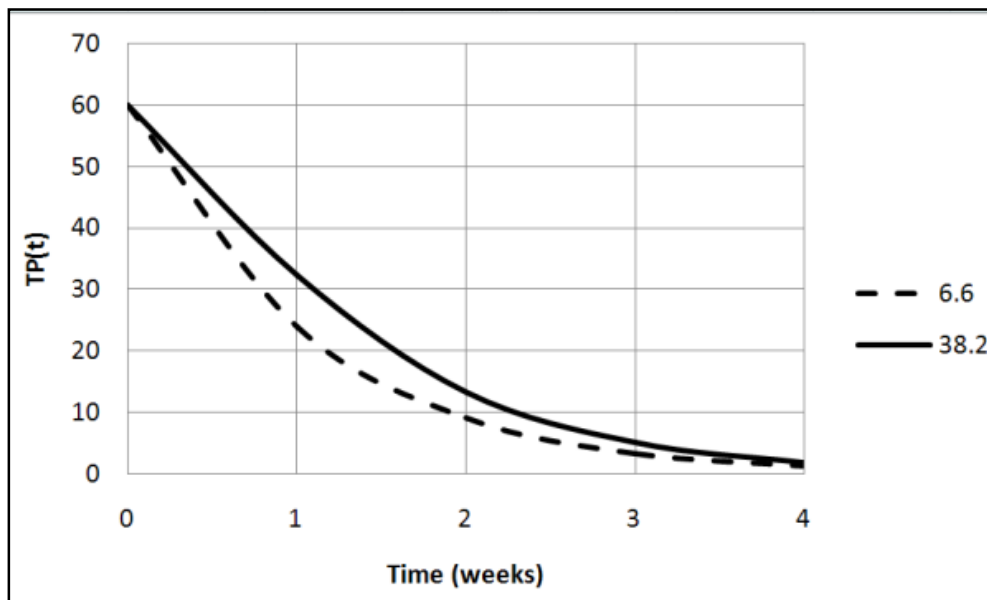
3.2.3. FURTHER CONCLUSIONS

The system proposed in Sec. 3.1 was found to experience a 90% reduction in the number of video streams during failure of one of its servers. This system is revisited in order to enhance the architecture and reduce this reduction. After several proposed modifications, it was shown that the system could tolerate the failure of one of its two servers, and operate with only a 14.3% (rather than a 90%) degradation in its number of supported video streams. As the proposed architectural modifications involve purchasing higher-end equipment, a performability analysis was conducted, to compare both reliability data with performance, indicating a relationship between buying higher-end equipment and also buying more reliable equipment.

Again, the control data experiences no over-delayed or dropped packets, the WiFi load is unaffected, and any degradation in the number of video streams does not reflect on the number of passengers with video screen capability. All runs are conducted with 33 seeds for statistical analysis.

3.3. FAILURE SEQUENCE PERMUTATIONS

3.3.1. TWO-WAGON ARCHITECTURAL AND FAULT-TOLERANCE ENHANCEMENTS

This section studies the two-wagon model, described in Sec. 3.1.2 and applies the enhancements proposed in the previous section that were found to give maximum performability. Using the newly proposed enhanced model, all possible failure sequences will be analyzed and simulated to study the system behavior in all possible states.

The enhanced two-wagon system can be seen in Fig. 16 with the enhanced components marked accordingly (dashed square and thickened connections indicate modified components). The remainder of the network architecture is unchanged (as described in Sec. 3.1.2).

Figure 16. Enhanced Two-Wagon Architecture [73]
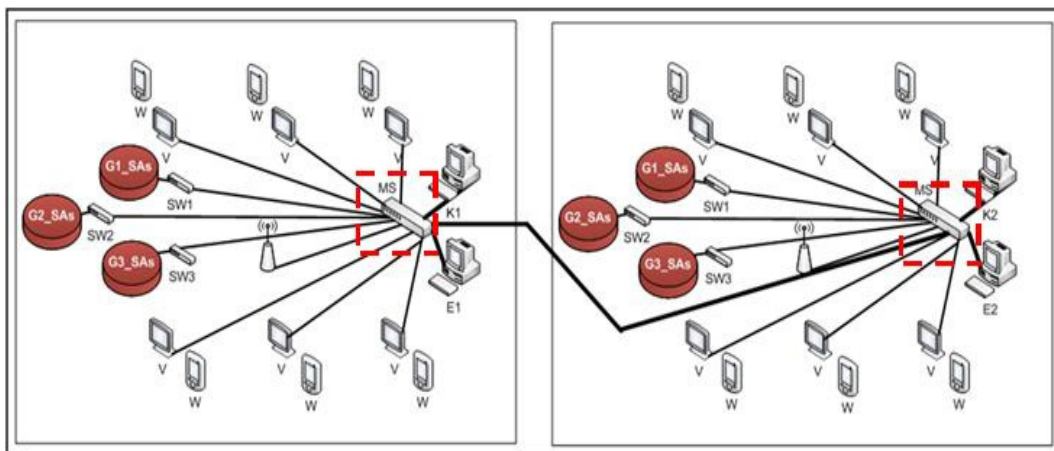
A new fault-tolerance philosophy is proposed in this section in order to improve performance compared to the previous fault-tolerance operation parameters proposed in Sec. 3.1.2. The two-wagon model, without any enhancements, had all sensors sending to all operational servers, for any machine to carry the load of its counterpart in the event of a failure. This imposed an extreme load on the network. This fault-tolerance *philosophy* is changed in this section to decrease network congestion and improve performance during the many different failure states. Due to the change in the philosophy, the sequence of failure will also matter.

There are now two wagons, hence four servers, two dedicated to control (Ks) and two dedicated to entertainment (Es). In order to decrease congestion on the network, each sensor will only send its samples to two servers at any point in time. This technique will guarantee that the appointed server for control is receiving its data as well as a counterpart with the most up-to-date data in the case of failure. In this section of the study, priority will be given to a control server assuming that it would have a lower failure rate than the entertainment servers. To more clearly describe the philosophy, an example where the failure sequence is $K_1K_2E_1E_2$ will be explained in detail. Initially, in the fault-free scenario, sensors will send their samples to both K_1 and K_2. Each K will be handling the control data for its own wagon. If (when) K_1 fails, K_2 will handle the full control load, and all sensors of wagon one will send their samples to both K_2 and E_1 and all wagon two sensors will send their samples to both K_2 and E_2. A similar analogous philosophy is applied to the entertainment load; whereby an entertainment server would be responsible for its entertainment counterpart and only when both entertainment servers have failed (or if the remaining entertainment server is unable to carry the full load of both wagons) would a control server begin to take on an entertainment load. The philosophies previously described are geared towards two goals:

1. Increasing reliability (by decreasing congestion and implementing fault-tolerance at the controller level)

2. Minimizing entertainment load degradation (during failure of one or more machines)

The next section describes the detailed set of scenarios and the simulations run.

3.3.2. FAILURE SCENARIOS

With a total of four servers, there are a total of 4! = 4×3×2×1 = 24 possible permutations, and hence a total of 24 possible failure sequences, as presented in Table 4. Scenario 1 in Table 3 can also be written: $K_1K_2E_1E_2$, where this is the order of failure: K_1 fails first and E_2 last, Note this table only shows 12 of the 24 permutations for the remaining 12 are identical except with the subscripts reversed (every 1 is replaced with a 2), for example, $K_1K_2E_1E_2$ becomes $K_2K_1E_2E_1$.

Table 4 – Possible Scenarios [73]

Scenario	1st	2nd	3rd	4th
1	K_1	K_2	E_1	E_2
2	K_1	K_2	E_2	E_1
3	K_1	E_1	K_2	E_2
4	K_1	E_2	K_2	E_1
5	K_1	E_1	E_2	K_2
6	K_1	E_2	E_1	K_2
7	E_1	K_1	E_2	K_2
8	E_2	K_1	E_1	K_2
9	E_1	K_1	K_2	E_2
10	E_2	K_1	K_2	E_1
11	E_1	E_2	K_1	K_2
12	E_2	E_1	K_2	K_1

After a significant number of simulations and several days of result collection, the summary of the results is presented in Table 5. This table relates the scenario number (column 1), the active servers in wagon 1 (W1) and wagon 2 (W2) and the maximum number of DVD streams supported (and the machine supporting the streams in brackets). The full control and WiFi loads are supported in all scenarios.

Table 5 – Active Servers vs. Supported Streams per Wagon [73]

Scenario	W1	W2	No. of DVD Streams (Machine)
1	K_1 & E_1	K_2 & E_2	60 (E_1) & 60 (E_2)
2	K_1 & E_1	K_2 only	120 (E_1) only
3	K_1 only	K_2 & E_2	120 (E_2) only
4	K_1 & E_1	E only	60 (E_1) & 60 (E_2)
5	E_1 only	K_2 & E_2	60 (E_1) & 60 (E_2)
6	K_1 & E_1	None	120 (E_1) only
7	None	K_2 & E_2	120 (E_2) only
8	E_1 only	K_2 only	120 (E_1) only
9	K_1 only	E only	120 (E_2) only
10	K_1 or E_1	K_2 or E_2	43 (K_1 or E_1) & 43 (K_2 or E_2)
11	K_1 or E_1	None	42 (K_1 or E_1) only
12	None	K_2 or E_2	42 (K_2 or E_2) only

The control load was deemed fully functional according to the benchmarks used in both previous sections, all packets traveling from Sensor to Controller to Actuator

within the corresponding sampling period (dependent on the SA group). If a single DVD stream is added to the 'maximum' presented in the previous table, the delays would violate the sampling period ceiling. Any row in the previous table stating K or E can be expanded into several scenarios so in effect a representative scenario of each of the 24 scenarios was simulated. Table 6 shows the maximum end-to-end delay for a packet traveling from any sensor to a control/entertainment server (S→K) and from the server to each actuator group (K→A). Again, all these are the results of 33 simulations and these are absolute maximums experienced in any of the 33 simulations. Several figures below (Figs. 17 to 20 specifically) show some screenshots of the OPNET results for some of the previous simulations.

Figure 17. Delay Sample – G1 (K to A) [73]
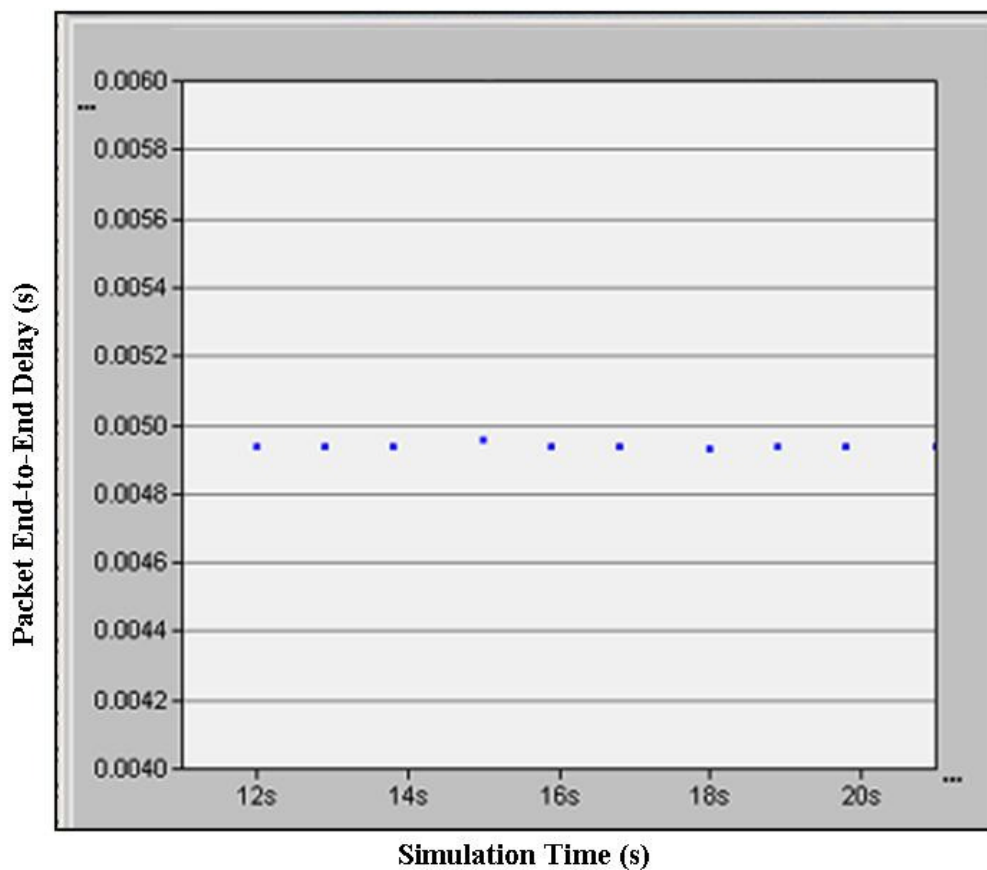
Figure 18. Delay Sample – G2 (K to A) [73]
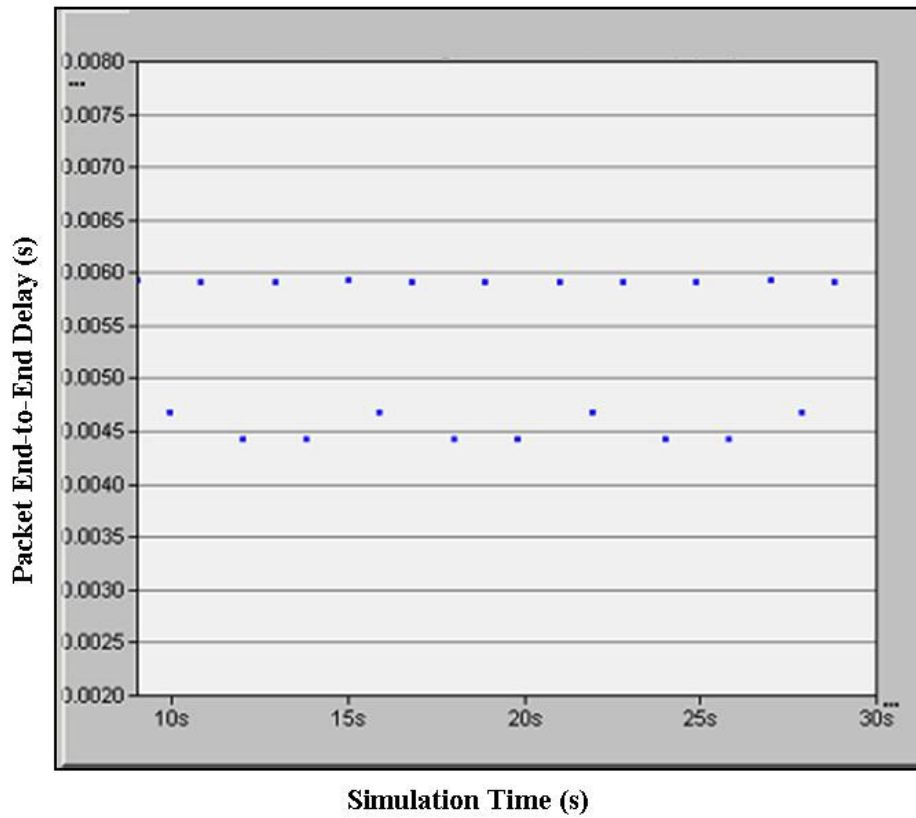
Simulation Time (s)

Figure 19. Delay Sample – G3 (K to A) [73]
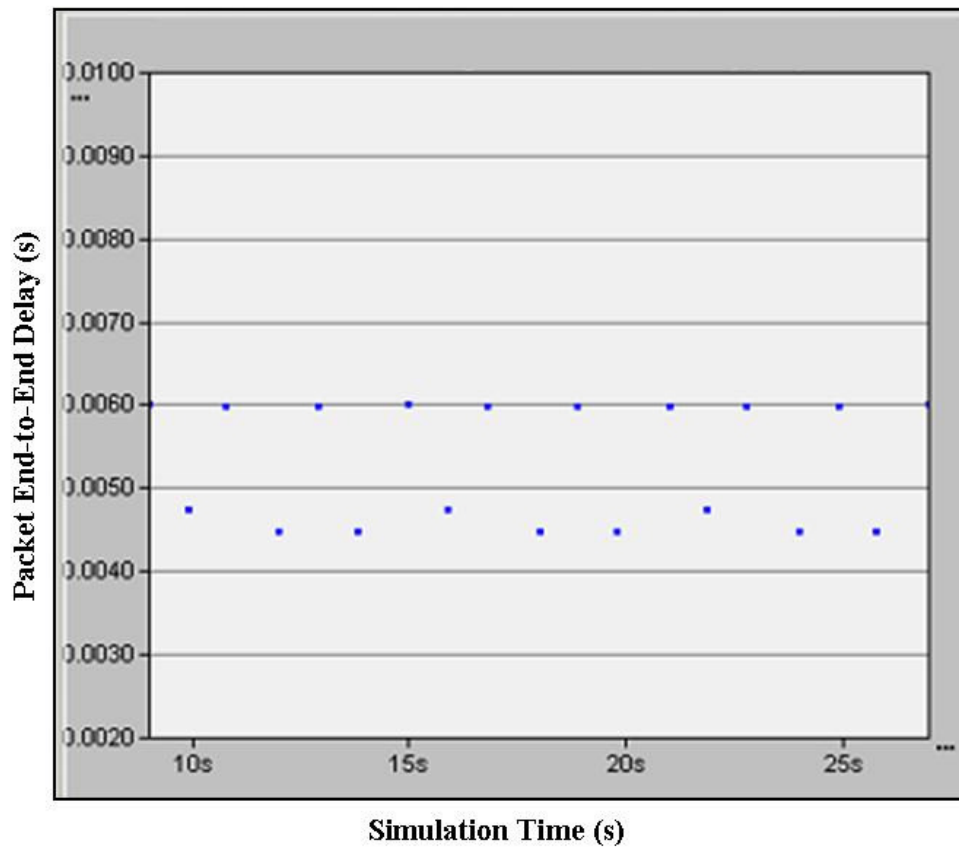
Simulation Time (s)

Figure 20. Delay Sample – S to K [73]
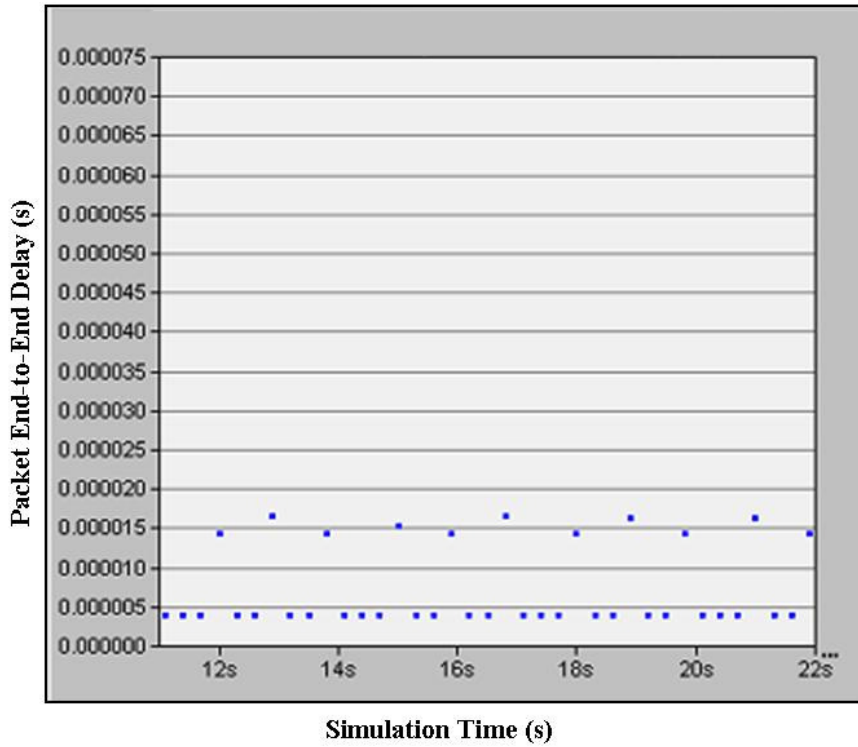
Simulation Time (s)

All graphs have an x-axis representing simulation time in minutes and seconds and a y-axis representing delay in seconds. Again, these are not the full duration of the simulation but a representative sample with visible resolution (as simulation time increases the graphs become cluttered and must be analyzed using spreadsheet software). These results conclude this study and a summary is presented next.

Table 6 – End-to-end Delay per Scenario [73]

#	S→K (ms)	K→A GP1 (ms)	K→A GP2 (ms)	K→A GP3 (ms)
1	0.0045	0.0086	0.0069	0.0057
2	0.0076	0.0085	0.0065	0.0057
3	0.0076	0.0093	0.0066	0.0056
4	0.0046	0.0077	0.0075	0.0057
5	0.0043	0.0085	0.0071	0.0060
6	0.0042	0.0143	0.0123	0.0097
7	0.0042	0.0142	0.0122	0.0099
8	0.0065	0.0085	0.0071	0.0054
9	0.0065	0.0085	0.0071	0.0054
10	0.0065	0.9525	1.5049	1.5395
11	0.0060	0.9111	1.4753	1.4910
12	0.0060	0.9110	1.4758	1.4913

3.4. SUMMARY

In the previous sections a NCS for use on-board of train-wagons under the umbrella of ITS, was studied. This NCS, used unmodified Switched Ethernet and WiFi as a shared backbone for both control and entertainment loads. Initially, the system is tested as a proof-of-concept to make sure that such sharing of a control load (with different sampling periods and S:A ratios) and an entertainment load (WiFi nodes and DVD quality video screens) will not result in over congestion of the network. The system is proved to be fault-tolerant at the server level, guaranteeing correct control operation with a degraded entertainment load (in both the single and two-wagon scenarios) with only one functional server (out of two or four depending on the number of wagons). The system is then enhanced to minimize entertainment degradation and a performability analysis is conducted to relate reliability models with performance (or reward). Finally the enhanced system is scaled up to two wagons and every possible failure sequence is simulated to find the maximum reward at each failure state. The search for maximum reward is aided by a new fault-tolerant philosophy that minimizes congestion while maintaining reliability. At any state, in any scenario, enhanced or unenhanced, all control packets are shown to arrive within their sampling period deadlines and with zero packets dropped after 33 simulations on OPNET Network Modeler.

4. WIRELESS NCS FOR INDUSTRIAL AUTOMATION

4.1. ENHANCED CELL CONCATENATION

4.1.1. INTRODUCTION

As was studied in [66], it is important for a WNCS workcell of any kind to be able to operate in close proximity with other workcells of the same system. However, in [66], there were certain limitations imposed upon the system due to channel reuse and subsequently the effects of co-channel interference. Of these limitations was a nonzero minimum inter-cell distance. This would mandate certain impositions on production line dimensions and hence restricts the application of such a system on both existing systems (to be upgraded) and new factories (to be built). It is hence critical to find a work-around to avoid this limitation. In order to find this work-around, the system must first be analyzed mathematically.

4.1.2. MATHEMATICAL ANALYSIS OF CONCATENATION TOPOLOGY

To analyze the system presented in [66] mathematically, the layout must be depicted in an illustrative figure. Figure 21 shows the intended concatenation with a zero meter inter-cell distance. The distances (labeled d and d_{min}) to be used in calculations are shown, representing the distance between the nearest co-channel interferer and the distance to the furthest node to be covered.

In [66], it was concluded that avoiding co-channel interference could be achieved via three methods:

1. Increasing distance between co-channel interferers (by increasing inter-cell distance).
2. Decreasing transmit power (to decrease coverage)
3. Increase Packet Reception Power Threshold (PRPT) (to decrease coverage)

The goal of the system being to minimize inter-cell distance, this removes point 1 from the possible solutions. Secondly, as the minimum WiFi transmit power (1mW, according to standard) is used (and for comparison with WISA), this also negates the possibility of decreasing transmit power. This leaves the third point and that is

modifying PRPT. This can be achieved using signal attenuators or ordering custom parts from network component manufacturers [75, 76].

Figure 21. Concatenation of Two Cells [74]
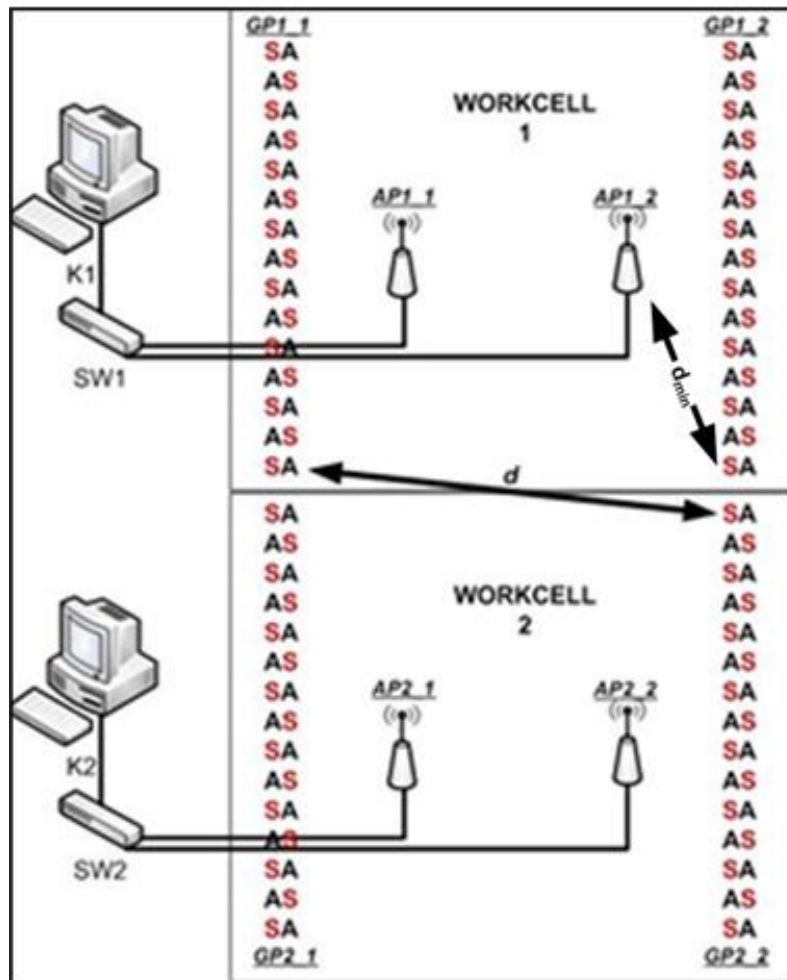
The default PRPT value of a WiFi node on OPNET Network Modeler is −95dBm. The study in [66] concluded that the PRPT of all nodes must be raised to −50dBm as well as employing a 2m inter-cell distance to sufficiently avoid co-channel interference. At this inter-cell distance, a higher PRPT would cause control packets dropped (within a single-cell) and a lower PRPT would cause co-channel interference. Several Propagation/Path-Loss models shall be used to analyze the transmission and reception qualities of the system.

In order to analyze the system, a simplification must be used as shown in Fig. 22, depicting a transmitter and a receiver.

Figure 22. Transmission/Reception Overview
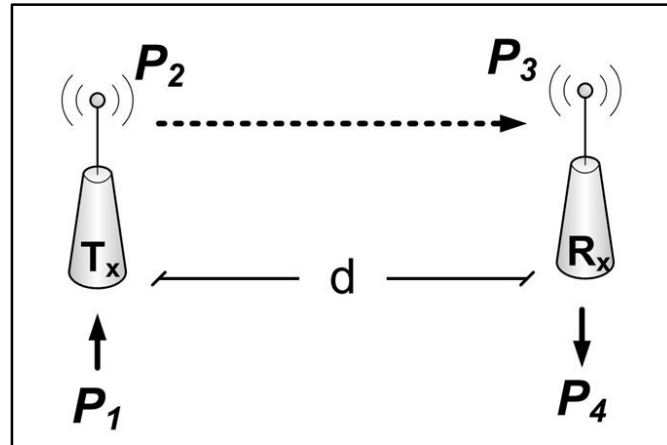
The transmitter and receiver represent two nodes and can be analyzed in two stages:

1. Two nodes within the same cell
2. Two nodes, one from each cell, operating with the same channel (co-channel interferers)

The implications of using each stage will determine the limits of the PRPT needed to achieve correct communication while sufficiently avoiding co-channel interference. This will become clearer in what follows.

The first model to be used is the Free-Space of Friis transmission/propagation model [77].

$$P_r = P_t G_t G_r (\lambda/4\pi d)^2 \qquad (1)$$

where $d = \dfrac{c/f}{4\pi\sqrt{P_r/P_t G_t G_r}}$

P_r is signal power (or strength) at R_x (W)

P_t is input power to T_x (W)

G_r is antenna gain at R_x

G_t is antenna gain at T_x

λ is signal wavelength (m)

c is speed of light (3×10^8 m/s)

f is operating frequency (ISM Band - 2.4GHz)

d is distance between T_x and R_x (m)

Using Fig. 22, the following can be stated:

1. $P_1 = P_t$
2. $P_2 = P_t G_t$
3. $P_3 = P_t G_t (\lambda/4\pi d)^2$
4. $P_4 = P_t G_t G_r (\lambda/4\pi d)^2$

In OPNET Network Modeler, transmit power is P_2 and P_3 can used to obtain PRPT. As previously stated, transmit power $P_2 = 1\text{mW}$ and for WiFi, $\lambda = 0.125\text{m}$. The distance between the T_x and the R_x being known, depends on whether calculating PRPT is to guarantee correct operation (SA to AP connectivity) or to avoid co-channel interference. For correct operation, based on cell dimensions, an AP (or an SA) **must** be able to cover a radius of at least 1.8m. Simultaneously, to avoid co-channel interference, the coverage **must** not extend beyond 2.8m, the minimum distance between any two nodes (SA or AP) from different cells, using the same WiFi channel. These two distance limits (1.8m and 2.8m) can be seen in Fig. 21, d_{min} and d respectively. In a single sentence, a workcell (all SAs, APs) must be able to communicate with their corresponding nodes while simultaneously being completely oblivious to the co-channel interferers. So, with all variables now known, the aim of solving the different propagation models is to find the PRPT values to satisfy the previously stated conditions and the equations become a function of $P_r(d)$.

Solving Eq. 1, with $d = 2.8\text{m}$ and 1.8m gives $P_3(2.8) = -49\text{dBm}$ and $P_3(1.8) = -45\text{dBm}$. These values represent received signal strength and a packet propagating through free space, would undergo signal attenuation. If the PRPT of a receiver is set at a value between $P_3(2.8)$ and $P_3(1.8)$, it should theoretically be able to communicate with its AP (or SA for in the case of an AP) while simultaneously, sufficiently avoiding interference. Packets arriving from a distance greater than 2.8m will have attenuated signal strength below the PRPT of the receiver and the packet will not be recognized, while packets arriving at a distance closer than 1.8m will be within PRPT limits and hence will be correctly recognized.

It is important to analyze the system using a more realistic model though, for the previously stated free space model is not pessimistic enough. One such model is the One-Slope Path-Loss model [78].

$$L(d) = L_0 + 10n \times \log(d) \qquad (2)$$

where:

$L(d)$ is path loss at distance d in meters (dB)

L_0 is experimentally measured reference: path loss at d_0 (dB)

n is the path loss exponent

Reference [78], presents a set of values for L_0 and n depending on the environment. The most relevant values presented in [78] are those relating to the WiFi operating frequency, n ϵ [1.2, 3.5, 4.2]. In free space, n = 2, and the higher the n the worse the signal attenuation. For n = 1.2, an indoor corridor, the model is actually less pessimistic than free space. Using these three values, path-loss is calculated for the two distances: 2.8m and 1.8m. The values are shown in Table 7.

The ITU Standard Indoor Propagation Model is also used to calculate the PRPT constraints [79].

$$L(d) = 37 + 30\log(d) + 18.3\, m^{\left(\frac{m+2}{m+1}-0.46\right)} \qquad (3)$$

where:

m is the number of floors between T_x and R_x in an office like environment

In this scenario, there are no floors between T_x and R_x so $m = 0$. The result of solving Eqs. 2 and 3 result in path-loss (dB) rather than signal strength and hence require further calculations to find PRPT (for both values of distance). The following equation can be used to obtain PRPT.

$$P_R = P_T - L(d) \qquad (4)$$

This equation is solved using a transmit power of 1mW (in dBm of course) and the calculated path loss, and the resulting value is the PRPT. The results of these calculations are presented in Table 7. The benefit of these calculations is a PRPT range, setting a PRPT within this range should guarantee correct performance and avoidance of co-channel interference.

Table 7 – PRPT **L**IMITS FOR **D**IFFERENT **M**ODELS **[74]**

Propagation/Path Loss Model	Min. PRPT (dBm)	Max. PRPT (dBm)
OPNET	−50	−50
Free Space	−49.0	−45.1
One-Slope $L_0 = 40.2$dBm, $n = 4.2$	−58.0	−50.9
One-Slope $L_0 = 40.2$dBm, $n = 1.2$	−45.5	−43.3
One-Slope $L_0 = 40.0$dBm, $n = 3.5$	−55.6	−48.9
ITU Indoor model	−50.4	−41.4

Observing the results it can be noted that the behavior of OPNET Network Modeler is closest to that of Free Space, which is a valid conclusion, considering the lack of fading/path loss models available in the license used for this research. The modeler however does give a single optimal value rather than a range for PRPT and this is acceptable for the sake of simulations. While the calculations show the required values of PRPT that may be needed to achieve 0m concatenation in a real implementation, the credibility of the simulator motivate a work-around.

4.1.3. CHANNEL ALLOCATION SCHEME AND MODELING INTERFERENCE

Rather than going through the process of avoiding co-channel interferers, Cisco Systems, Inc. suggest the use of four WiFi channels that have minimal frequency overlap [80]. These four channels are: Ch1, Ch4, Ch8 and Ch11. The suggestion also recommends the system architecture to be as follows in Fig. 23.

As there is a frequency overlap between Ch1 and Ch4, and also between Ch8 and Ch11, the shown layout minimizes coverage overlap between the interfering channels. When this allocation is used, precautionary measures used in [66] to lock the reused channel shall be implemented on all four channels. These four channels are inaccessible to any nodes outside the WNCS. As there is a frequency overlap between Ch1 and Ch4, and also between Ch8 and Ch11, the shown layout minimizes coverage overlap between the interfering channels.

Figure 23. New Channel Allocation Scheme [74]
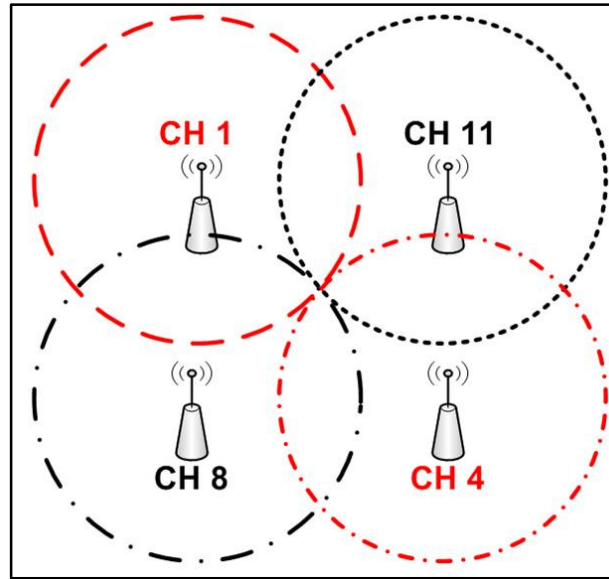
When this allocation is used, precautionary measures used in [66] to lock the reused channel shall be implemented on all four channels. These four channels are inaccessible to any nodes outside the WNCS. Using password access, limiting the number of IPs and not broadcasting the SSID prevents users from outside the WNCS from accessing the channels. However, a service engineer wanting to communicate with the controller needs a wireless route (as well as to study the resilience to interference exhibited by the new system). A fifth access point is placed in the center of the two cells operating on any of the neighboring channels (2, 3, 5, 6, 7, 9, 10) to study the effect of interference. The wireless node is made to rotate around the entire two-cell model while communicating with the controller. The effects of this model will be presented in the results section.

4.1.4. SIMULATED LAYOUTS AND RESULTS

This study attempts to model two different topologies: 0m concatenation and an L-shape architecture. Frequently in a production line, conveyer belts go through direction changes and a right angle turn is needed. This study aims to model both of these topologies. Figs. 24 and 25 show the two topologies as well as the route taken by the alien node, circling the system.

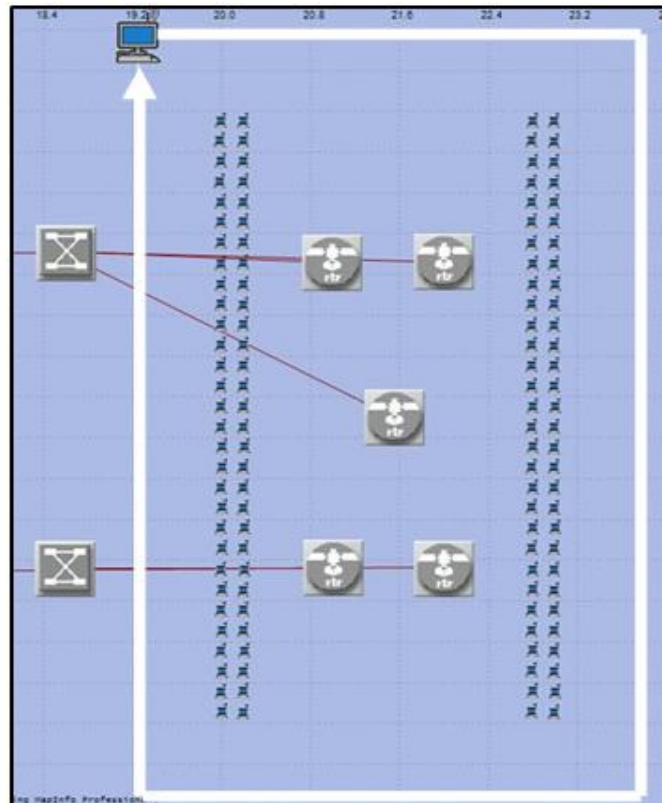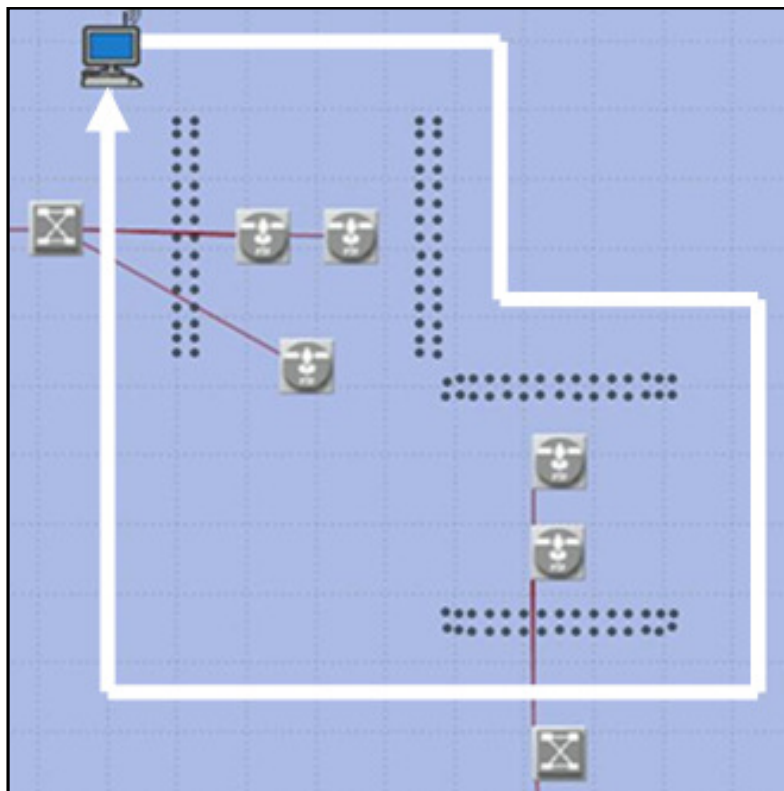**Figure 24. 0m Concatenation [74]**

Figure 25. L-Shape Concatenation [74]

The models used in the simulation are:

1. Sensors, Actuators, Service Engineer: WLAN Workstation Advanced

2. Controllers: Ethernet Workstation Advanced

3. Wireless Access Points: WLAN Ethernet Router Advanced

4. Switches: Ethernet Switch Advanced

After a set of simulations testing both topologies in the absence and existence of interference (a FTP file size ranging from 1KB to 6.5KB) it was shown that the system can tolerate a certain amount of interference while maintaining correct packet transmission/reception and acceptable delays. These delays are shown in the table below and are subjected to a 95% confidence analysis.

Table 8 – End-to-end Delay Results per Scenario [74]

Scenario	Max. delay range [μ−Δ; μ+Δ] S→K (ms)	Max. delay range [μ−Δ; μ+Δ] K→A (ms)
In-line 0m – Noiseless	[0.81; 0.89]	[3.10; 3.78]
L-shape – Noiseless	[0.84; 0.95]	[3.39; 3.90]
In-line 0m – Noise[a]	[1.89; 2.10]	[7.78; 9.46]
L-shape – Noise[a]	[1.16; 1.28]	[6.14; 7.71]

a. Noise modeled over channels: 2, 3, 5, 6, 7, 9, 10

Logically the L-shape orientation performs with lower delays than the 0m concatenation due to the increased distance between co-channel interferers.

4.1.5. INITIAL CONCLUSIONS

Using a non-traditional channel allocation scheme, the previous module of this thesis simulated and proved that concatenating two WiFi WNCS workcells is possible at a previously unachievable distance of 0m. The study also modeled a right-angle turn in the conveyer belt of the production line.

The modeled scenarios were subjected to WiFi interference on channels neighboring those of the control system. The results of the study show that with the new channel allocation scheme, the previously untested models can operate correctly

in the absence and existence of interference while maintaining packet end-to-end delays below the 16ms per link benchmark set in [65] and with zero packets lost with a FTP file size of up to 6.5KB. All results presented are subjected to a 95% confidence analysis.

4.2. INITIAL FAULT-TOLERANCE ENHANCEMENTS

4.2.1. FAULT-TOLERANCE PHILOSOPHY

As was presented in Sec. 2.6.3, it is a logical step to take advantage of neighboring cells for fault-tolerance [67]. Fault-tolerance was incorporated at the controller level by wiring the two workcell switches together. Each sensor was made to send its data to both controllers and the controllers were to exchange a watchdog signal. A sensor would sample the plant, generate two copies of the packet and send one to each controller. Each controller processes the information and prepares the control word. However, only the designated controller actually sends the control word to the designated actuator. In the event of the failure of either controller, the neighbor will take over. The system philosophy used, utilized a wired connection between the two workcells. It would be a much more appealing system if the workcell could be wirelessly connected to its neighbor. Such a scenario would give the system freedom to enable fault-tolerance around different orientations and with less cabling, thereby remaining consistent with the term *Wireless* NCS [81].

4.2.2. PROPOSED MODEL

The system studied in [66] will be used as the foundation for this section of the study. While Sec. 4.1 proposed a work around for 0m workcell concatenation, the more traditional allocation scheme will be tested first. As shown in Fig. 26, a 3m inter-cell distance is imposed between workcells. Each workcell now has three access points, the third being dedicated to the fault-tolerance communication. As there is a need for a third access point, it is decided that each workcell be designed as an individual unit in such a way as to enable concatenation and fault-tolerance with minimal interference. As such, the three non-interfering WiFi channels (1, 6 and 11) are fully utilized by a single workcell.

47

Figure 26. Wireless Fault-Tolerance Architecture [81]
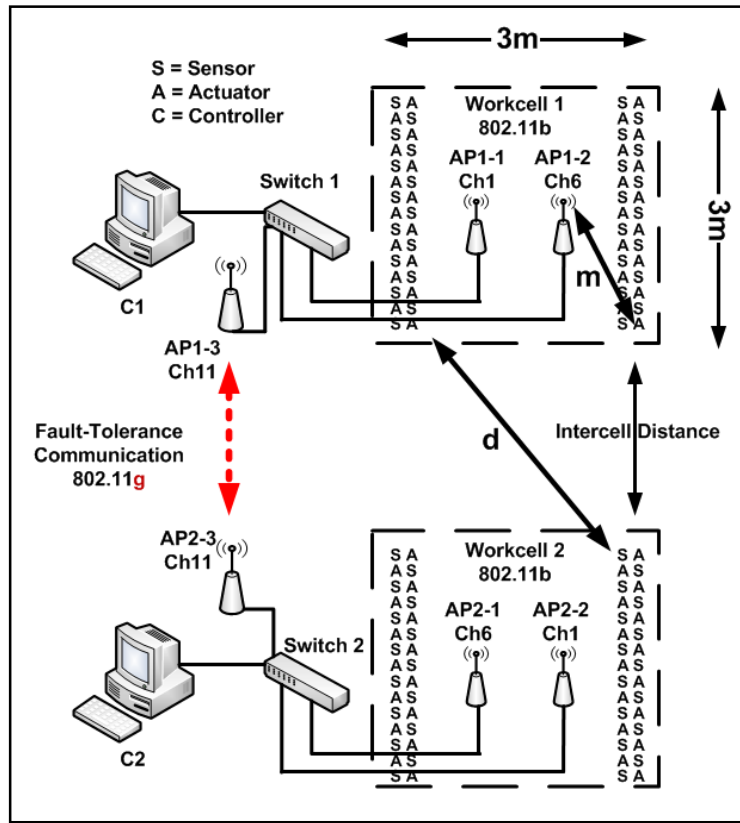
While Ch11 is reused between both cells, this is for inter-cell communication and is not deemed co-channel interference (unlike Ch1 and Ch6). As in all concatenated models a PRPT of −50dBm and a 1mW transmit power are used. However, as Ch11 is not under a threat of co-channel interference and needs to maximize coverage to communicate between cells, default PRPT is used (−95dBm).

Initially, the bottleneck imposed by the Ch11 access points (FT APs) was not expected and the model was built in OPNET. Immediately, it was clear that the amount of traffic of a single cell (without duplication of packets by the sensors) let alone two cells would be far too much for the single FT AP per cell to handle for intercommunication. This realization mandated either an abandonment of the idea of *wireless fault-tolerance* or an increase in bandwidth which would call for a change of protocol. The solution presents itself in the form of IEEE 802.11g [61], which offers a higher bandwidth at the sake of reduced coverage. The reduced coverage however is

not much of a threat in the small distances within a factory-floor and hence it was not a disadvantage.

The FT APs were selected to operate using 802.11g rather than 802.11b, to utilize a data rate of 54Mbps rather than 11Mbps. The next section discusses the simulated scenarios and the results of the simulations.

4.2.3. SIMULATED SCENARIOS AND RESULTS

As shown in Fig. 26, the system was built on OPNET Network Modeler and was simulated in four stages: Noise-free fault-free, noise-free faulty, noisy fault-free, noisy faulty. Similarly to [66], reused channels (Ch1 and Ch6) are locked and hence interference is simulated on Ch11. Results to the various simulations conducted are summarized in Table 9.

Table 9 –Maximum End-to-end delay ranges [μ−∆; μ+∆] [81]

Scenario	Max FTP (KB)	Max Delay S→K (ms)	Max Delay K→A (ms)
1 Cell [70]	0	[1.50; 1.64]	[2.23; 2.90]
1 Cell - Noise[70]	40	[1.62; 1.75]	[14.07; 14.67]
2 Cells [71]	0	[0.66; 0.71]	[2.99; 3.53]
2 Cells - Noise [71]	40	[1.06; 1.13]	[11.99; 12.65]
Fault-Free [81]	0	[1.41; 1.49]	[9.76; 11.01]
Fault-Free – Noise [81]	300	[2.93; 2.99]	[10.28; 11.41]
Faulty [81]	0	[0.70; 0.73]	[4.99; 5.79]
Faulty – Noise [81]	500	[1.72; 1.75]	[9.41; 10.30]

The decrease in end-to-end delays for the faulty scenario is found here also, as in [67], and this is due to the absence of duplication of sensor packets. Several OPNET screenshots show the delays below: Figs. 27 to 30. As usual, the x-axis represents simulation time (in minutes and seconds) and the y-axis the delay (in seconds). Again, these are just some samples of delay for a short interval, not for the full duration of simulation.

Figure 27. Faulty Scenario without Noise (S to K) [81]

Simulation Time (minutes & seconds)
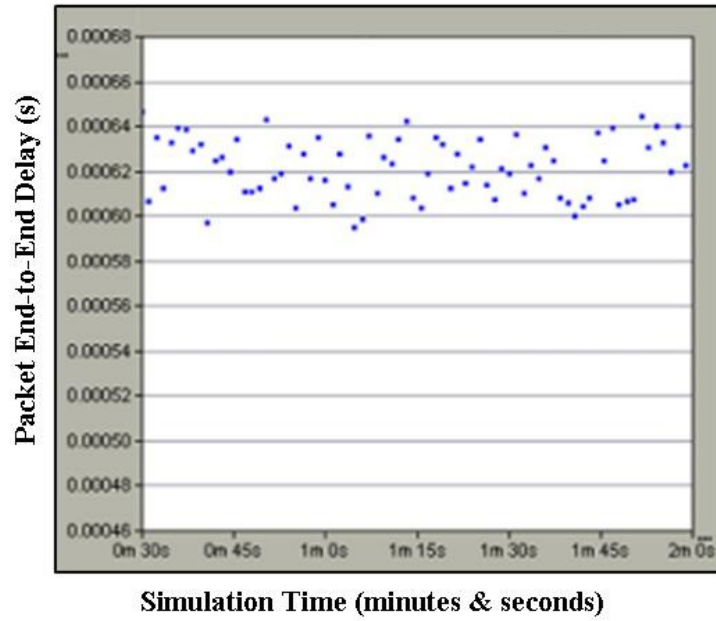
Figure 28. Faulty Scenario without Noise (K to A) [81]

Simulation Time (minutes & seconds)
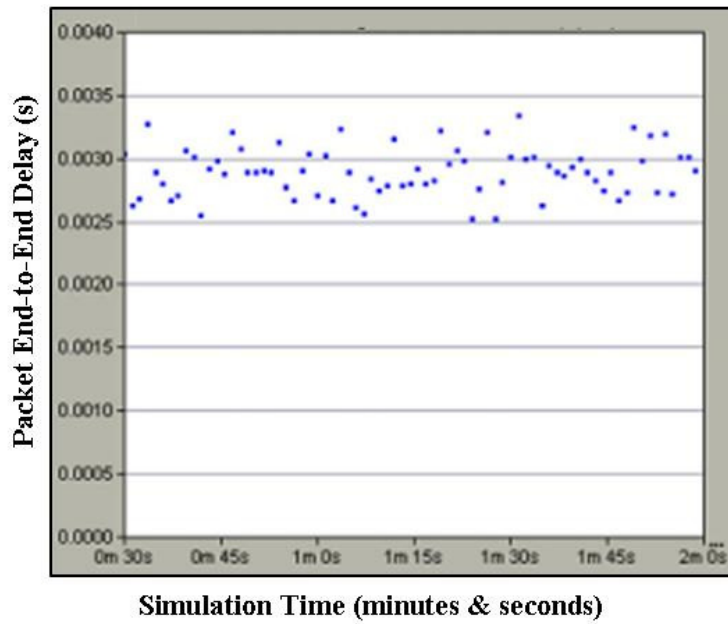
Figure 29. Faulty Scenario with Noise (S to K) [81]

Simulation Time (minutes & seconds)
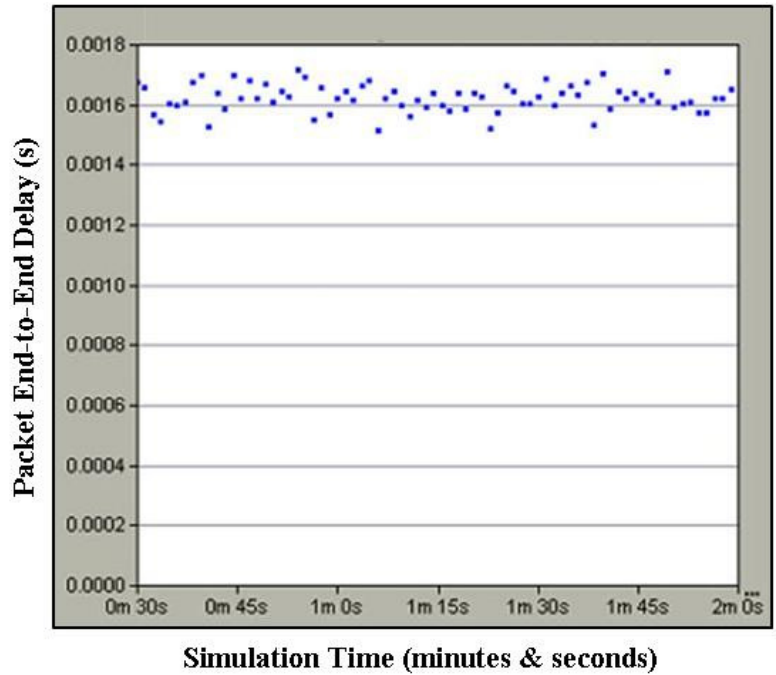
Figure 30. Faulty Scenario with Noise (K to A) [81]

Simulation Time (minutes & seconds)
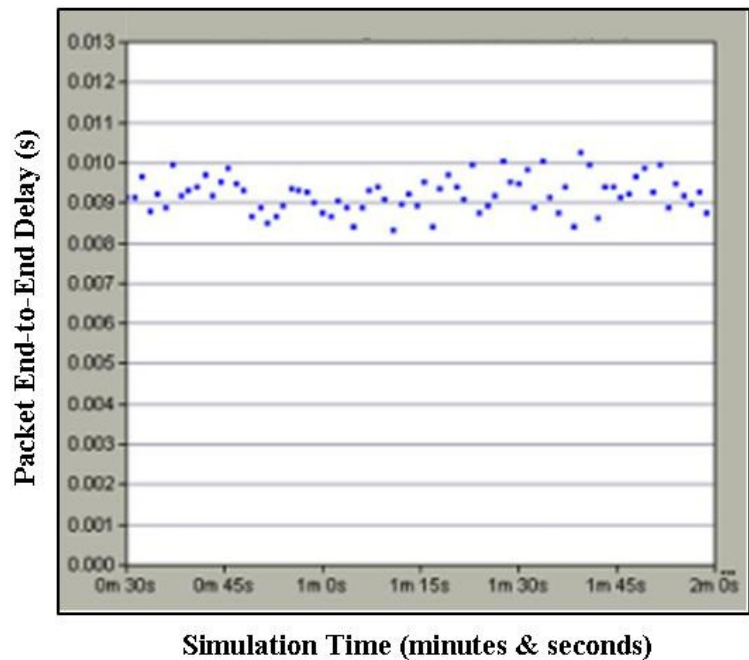
The delay increase after simulating interference is notable comparing Figs. 27 and 29 to 28 and 30. All delays presented in Table 9 have been subjected to a 95% confidence analysis and guarantee zero packets lost.

4.2.4. Initial Fault-Tolerance Conclusions

The concept of wireless fault-tolerance was successfully simulated with correct packet transmission/reception in the presence of noise. The addition of IEEE 802.11g to the system enabled the wireless intercommunication between cells to occur efficiently, making use of the increased data rate. However, the system was simulated with an inter-cell distance of 3m, and was forced to utilize channel reuse. The introduction of IEEE 802.11g to the system motivated the next section of the study, rather than studying wireless fault-tolerance with the new channel allocation scheme proposed in the previous section. The reasons for this shift shall become clear in the following section.

4.3. Migrating to IEEE 802.11g and Performability Analysis

4.3.1. Introduction

This section of the study introduces a significant modification to the system proposed in all the previous sections. That modification is the departure from IEEE 802.11b to a total utilization of IEEE 802.11g for the same reasons mentioned in the previous section [82]. There are a number of added benefits to this migration that will be revealed in the following sections.

4.3.2. Proposed System

The single-cell model retains all but one aspect: the number of and protocol used by the WiFi access points. Specifically, now that all nodes within the workcell utilize IEEE 802.11g, a single access point can now support all SAs within the workcell due to the increased data rate. This has several benefits. Firstly, the increase in data rate allows a significant reduction in delays and noise/interference resilience. Secondly, the existence of a single access point per cell allows the cascading of up to three cells, with zero meter inter-cell distance without the need for channel reuse. Thirdly, due to the increase in data rate, the system can withstand triplication of sensor data and hence, wired fault-tolerance at the controller level using the same philosophies stated

earlier will no longer experience a bottleneck due to the WiFi channel being over-congested. Figs. 31, 32 and 33 show the intended models to be simulated.

Figure 31. Single-Cell Model [82]

Figure 32. Two-Cell Model [82]

Figure 33. Three-Cell Model [82]
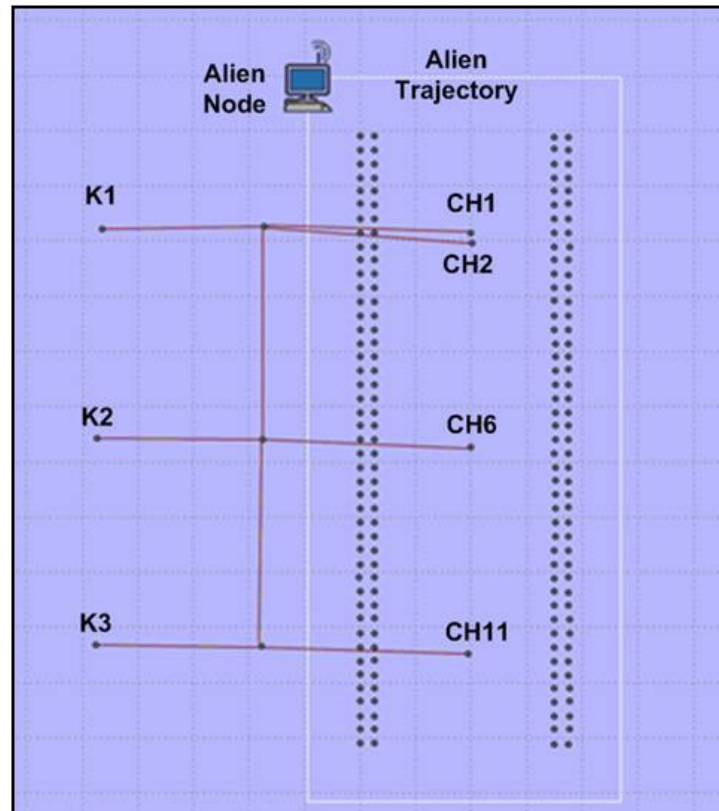
4.3.3. SIMULATED SCENARIOS AND RESULTS

The simulation set for this section is the largest of all three WNCS modules presented in this thesis:

1. Single Cell – Noiseless
2. Single Cell – Noisy
3. FT Two Cells – Fault-Free, Noiseless
4. FT Two Cells – Fault-Free, Noisy
5. FT Two Cells – Faulty, Noiseless
6. FT Two Cells – Faulty, Noisy
7. FT Three Cells – Fault-Free, Noiseless
8. FT Three Cells – Fault-Free, Noisy
9. FT Three Cells – Faulty (1 Failed K), Noiseless
10. FT Three Cells – Faulty (1 Failed K), Noisy
11. FT Three Cells – Faulty (2 Failed Ks), Noiseless
12. FT Three Cells – Faulty (2 Failed Ks), Noisy

54

Due to the use of triplication and the possible sensitivity of the channels 1, 6 and 11, interference will be modeled on neighboring channels as in [74], using a fourth AP located nearest to its most affected channel. This can be further understood by observing Fig. 33 showing the AP using Ch2, situated nearest to the AP using Ch1.

The results of all simulations have been included in Table 10. All results are subjected to a 95% confidence analysis, guaranteeing zero packets lost and delays with the 16ms per link benchmark. It is important to explain that scenario 3C – 2F (3 Cell model, 2 controllers have failed) can tolerate a higher FTP file size compared to the single-cell model, and this is due to the increased distance the interfering node would be for most of its trip around the workcell. The exact value of the file size is merely a metric to gauge performance and is extremely optimistic. A real application requires further testing and observation.

Note FF means Fault-Free, 1F means one controller failed and 2F means two controllers failed.

Table 10 – MAX END-TO-END DELAYS PER SCENARIO VS. FTP FILE SIZE [82]

Scenario	Max FTP (KB)	S→K Delay (ms)	K→A Delay (ms)
1C	0	[0.074; 0.079]	[0.392; 0.504]
1C – Noise	240	[4.615; 5.010]	[11.142; 12.086]
2C – FF	0	[0.102; 0.118]	[1.735; 1.836]
2C – FF – Noise	220	[4.095; 4.742]	[9.612; 10.745]
2C – 1F	0	[0.102; 0.108]	[1.792; 1.922]
2C – 1F – Noise	230	[4.397; 5.158]	[10.363; 11.730]
3C – FF	0	[0.342; 0.552]	[1.398; 1.682]
3C – FF – Noise	120	[2.927; 3.291]	[11.700; 13.044]
3C – 1F	0	[0.104; 0.111]	[0.663; 0.799]
3C – 1F – Noise	220	[3.235; 3.548]	[10.184; 11.063]
3C – 2F	0	[0.073; 0,076]	[0.493; 0.629]
3C – 2F – Noise	300	[2.963; 3.418]	[7.844; 8.932]

4.3.4. PERFORMABILITY ANALYSIS

Finally, the two and three cell models presented in the previous subsection were subjected to a performability analysis. Figs. 34 and 35 show the CTMC for the two and three-cell models.
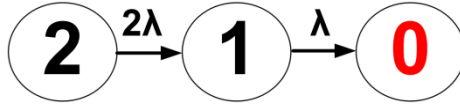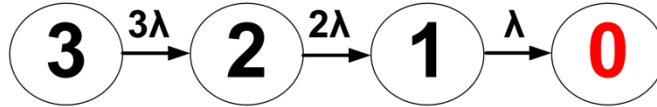
Figure 34. Two-Cell CTMC [82]

Figure 35. Three-Cell CTMC [82]

The state number represents the number of operational controllers and it is assumed that all controllers have the same failure rate λ. The main difference between this system and the fault-tolerant system presented in Sec. 3.2 is in system performance during failure. As described in Sec. 3.2.2, there is a need to define reward to calculate performability. In this system, yield or reward, is unchanged in terms of output. Unlike the train system, the control system experiences no drop in packets or violations in delays during failure of one (or two controllers in the three-cell system). Due to these attributes, a different metric must be used to define reward. All models were re-run with a single interference file size of 100KB for the sake of comparison and it was found that delays were a changing parameter.

In this analysis, it was decided that reward would be defined as the difference between the average end-to-end delay per link and the 16ms benchmark. This translates to a measure of the system robustness, the larger the difference between the delay and the benchmark, the more robust the system. Again, similarly to Sec. 3.2.2, the transient probability of residing at any of the CTMC states as a function of time can be calculated using the CK equations [34]:

$$\frac{d\boldsymbol{P}}{dt} = \boldsymbol{P} \times \boldsymbol{T} \qquad (1)$$

$$\boldsymbol{P} = (P2 \quad P1 \quad P0) \qquad (2)$$

$$T = \begin{bmatrix} -2\lambda & 2\lambda & 0 \\ 0 & -\lambda & \lambda \\ 0 & 0 & 0 \end{bmatrix} \qquad (3)$$

At system start up $t = 0$, $P_2(0) = 1$, $P_1(0) = P_0(0) = 0$. The CK equations can be solved as follows:

$$P_2(t) = e^{-2\lambda t} \qquad (4)$$

$$P_1(t) = 2\lambda(e^{-\lambda t} - e^{-2\lambda t}) \qquad (5)$$

$$P_2 + P_1 + P_0 = 1 \qquad (6)$$

Next, $TP(t)$ can be calculated using:

$$TP(t) = \sum_{i \in \psi} P_i Rew_i \qquad (7)$$

where ψ represents the various states of the CTMC and Rew_i is the reward as defined in the earlier at each state. Using the same techniques, the equations for transient probability for a three-cell model can be found as follows:

$$P_3(t) = e^{-3\lambda t} \qquad (8)$$

$$P_2(t) = 3\lambda(e^{-2\lambda t} - e^{-3\lambda t}) \qquad (9)$$

$$P_1(t) = 3\lambda(e^{-3\lambda t} - 2e^{-2\lambda t} + e^{-\lambda t}) \qquad (10)$$

$$P_3(t) + P_2(t) + P_1(t) + P_0(t) = 1 \qquad (11)$$

The reward is the summation of the difference between average delay per link and the 16ms benchmark, for both links. Each individual link reward has been labeled r_{SK} (difference between delay in link from sensor to controller and benchmark) and r_{KA} (difference between delay in link from controller to actuator and benchmark). The resulting reward is the summation of these two values. All these results are based on a 95% confidence analysis. The rewards for each case can be seen in Table 11.

Table 11 – REWARD PER STATE [82]

Scenario	FTP (KB)	r_{SK} (ms)	r_{KA} (ms)	Rew_i (ms)
3	100	13.82	7.43	21.253
2	100	14.57	11.23	25.796
1	100	14.96	12.77	27.721

Transient Performability as a function of time is presented in Fig. 36 using the three-cell model for different failure rates (0.5 and 1 failure/week) showing the main

advantage of performability: The quantitative assessment of reliability, performance and cost-effectiveness.

Figure 36. Transient Performability for Different Failure-Rates [82]
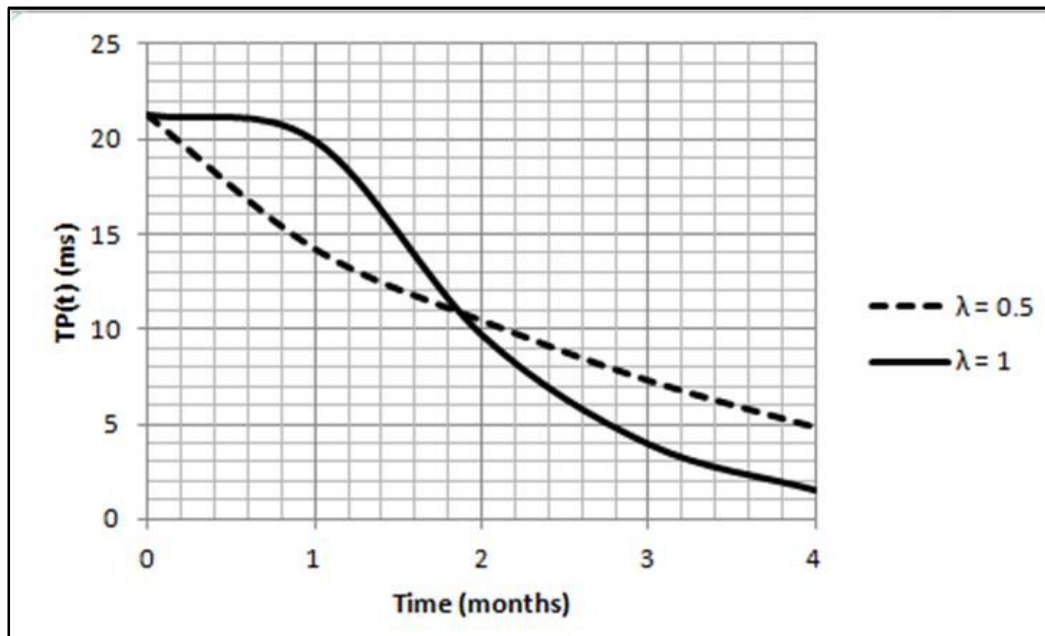
While a typical system would exhibit a consistently higher performability for a lower failure rate, this system does not for the following reason. Prior to 2 months of operation, while the highest transient probability is that of state 3, the equation has a significant weight (reward) given to the later states (states 2 and 1) due to the unique definition of reward presented in this study. However, as time progresses beyond the 2 months, the transient probabilities begin to counteract the effect of the reward and a more typical behavior is shown.

4.4. SUMMARY

This study presented a significant set of modifications to the WiFi WNCS system presented in [70–72], achieving 0m concatenation, a right angle turn in the conveyer, wireless fault-tolerance and up to three cascaded fault-tolerant cells. The study also subjected its final and most efficient model to a performability analysis showing the relationship between reliability and system performance. The final model shows that a system utilizing strictly unmodified IEEE 802.11g and 802.3 can tolerate the failure

of up to two of three controllers while guaranteeing correct performance in the existence of interference. The system end-to-end delays also surpassed those set by the existing solution (WISA) used as a benchmark for comparison.

5. CONCLUSIONS

This thesis presented two different applications of Networked Control Systems: Intelligent Transportation Systems and Industrial Automation. In both applications, a standard, unmodified IEEE communication/network protocol is used. The goal of the thesis was to prove, via simulation, that the proposed networked control systems are feasible solutions to the two applications presented. Different metrics are presented to gauge the performance of both systems and different benchmarks are used for comparison. All scenarios are simulated using OPNET Network Modeler and results are subjected to a 95% confidence analysis.

The conclusions of the study can be split into two parts (one for each application). In the case of networked control systems on-board of train-wagons, three modules of the study proved that an Ethernet and WiFi backbone spanning up to two train-wagons can be used to model a fault-tolerant (at the server level) system where the entertainment control loads are sharing the same networked control system. The fault-tolerance shows that the two wagons can operate with minimal performance degradation during the failure of up to three of four servers while maintaining correct packet transmission/reception and delays within system requirements. The control load experiences no losses or over delayed packets.

In the case of WiFi based wireless networked control systems, a previously studied model is completely redesigned to enable cascading of multiple cells, wireless fault-tolerant inter-cell communication and fault-tolerance of up to three neighboring controllers. The system is compared with an existing solution available in the market, using a modified, non-standard communication protocol. The results show that the proposed model (utilizing off-the-shelf equipment) surpasses the existing solution on a number of levels.

It is important to note that all studies were conducted on one of (if not the most) the most realistic and proprietary network simulators available. However, all findings must be reinvestigated in hardware implementations prior to using results as is.

APPENDIX – CONFIDENCE ANALYSIS

All results subjected to a confidence analysis follow the following calculations. Let:

X: random variable (maximum end-to-end delay).

μ: Average of X

σ^2:   Variance of X

X_i: sample of X obtained during i[th] OPNET simulation (using different seed)

n: No. of OPNET simulations

x: Sample mean

s^2:   Sample variance

$$x = \frac{1}{n}\sum_{i=1}^{n}X_i \qquad\qquad (1)$$

$$s^2 = \frac{1}{n-1}\sum_{i=1}^{n}(X_i - x)^2 \qquad\qquad (2)$$

OPNET Network Modeler requires a 'seed' value in order to initialize different random number generator equations that determine the different behavior or non-deterministic aspects of the simulation. Based on the Central Limit Theorem (CLT), if the distribution of a random variable is unknown, the distribution of its sample mean will approach a normal distribution, as the number of samples increases. The sample mean also approaches the ensemble mean and the variance of the sample mean is a scaled version of the ensemble mean (mean of $x = \mu =$ mean of X and variance of $x = \sigma_x^2 = \frac{\sigma^2}{n}$ where $\sigma^2 =$ variance of X [36, 37]. With the previous conditions, the confidence level is defined as the probability that x is below a certain distance from μ:

$$z = \frac{x - \mu}{\sigma_x} \qquad\qquad (3)$$

z: is a normal random variable (mean= 0 & variance = 1).

$$P(-z_\alpha < z < z_\alpha) = \alpha \tag{4}$$

$$P\left[\frac{|x - \mu|}{\sigma_x} < z_\alpha\right] = \alpha \tag{5}$$

By using 33 simulations, $n > 30$ and hence the sample standard deviation s can be used instead of σ as it is difficult to find $\sigma_x = \frac{\sigma}{\sqrt{n}}$. The Normal distribution will be used and z_α is calculated for a confidence level $\alpha = 95\%$.

REFERENCES

[1] J. Nilsson, Real-Time Control Systems with delays, PhD thesis, Department of Automatic Control, Lund Institute of Technology, Lund, Sweden, 1998.

[2] T. Skeie, S. Johannessen, and C. Brunner, "Ethernet in substation automation," IEEE Control Syst., Vol. 22, No. 3, 2002.

[3] F.-L. Lian, J.R. Moyne, and D.M. Tilbury, "Networked Control Systems Toolkit: A simulation package for analysis and design of control systems with network communication," Tech. Rep., UM-ME-01-04, 2001.

[4] C.M. Krishma and K.G. Shin, "Real-Time Systems," McGraw-Hill International Edition, 1997

[5] S. Bennet, Real-Time Computer Control: An Introduction, 2nd Ed., New York : Prentice Hall, 1994.

[6] J.P. Thomesse, "Fieldbus Technology in Industrial Automation," Proceedings of the IEEE, Vol. 93, No. 6, June 2005.

[7] Bosch, "CAN specification version 2.0," ISO 11898, 1991.

[8] "CAN in passenger and cargo trains," CAN in Automation, Available: http://www.can-cia.org/.

[9] "Overview of current automotive protocols," Vector CANtech Inc., 2003, Available: www.vector-cantech.com.

[10] B.P. Upender, "Analyzing the Real-time characteristics of Class C communications in CAN through Discrete Event Simulations," Advanced Digital Systems, United Technologies Research Center

[11] Official site for PROFIBUS and PROFINET: http://www.profibus.com/.

[12] IEEE 802.3 Standard.

[13] J.D. Decotignie, "Ethernet-Based Real-Time and Industrial Communications," Proceedings of the IEEE, Vol. 93, No. 6 2005.

[14] G. Marsal, "Evaluation of time performances of Ethernet-based automation systems by simulation of high-level Petri Nets," PhD Thesis, Ecole Normale Superieure De Cachan, December 2006.

[15] M.Felser, "Real-Time Ethernet – Industry prospective," Proceedings of the IEEE, vol. 93, no. 6, June 2005.

[16] F.-L. Lian, J.R. Moyne, and D.M. Tilbury, "Performance evaluation of control networks: Ethernet, ControlNet, and DeviceNet," IEEE Control Systems Magazine, vol. 21, no. 1, February 2001.

[17] B. Lounsbury and J. Westerman, "Ethernet: Surviving the Manufacturing and Industrial Environment," Allen-Bradley white paper, May 2001.

[18] S.H. Lee and K.H. Cho, "Congestion Control of High-Speed Gigabit-Ethernet Networks for Industrial Applications," Proceedings of the IEEE International Symposium on Industrial Electronics ISIE, Pusan, Korea, 2001.

[19] J.S. Meditch and C.T.A. Lea, "Stability and Optimization of the CSMA and CSMA/CD Channels." IEEE Trans. Comm., Vol. 31, No. 6, 1983.

[20] EtherNet/IP Performance and Application Guide, Allen-Bradley, Rockwell Automation Application Solution.

[21] J. Ferreira, P. Pedreiras, L. Almeida, and J. Fonseca, "Achieving Fault-Tolerance in FTT-CAN," Proceedings of the IEEE International Workshop on Factory Communication Systems WFCS, Vasteras, Sweden, August 2002.

[22] P. Pedreiras, L. Almeida, and P. Gai, "The FTT-Ethernet protocol: Merging flexibility, timeliness and efficiency," Proceedings of the IEEE Euromicro Conference on Real-Time Systems ECRTS, Vienna, Austria, June 2002.

[23] K. Steinhammer and A. Ademaj, "Hardware implementation of the Time-Triggered Ethernet controller," Embedded System Design: Topics, Techniques and Trends, Vol. 231. Springer Boston, 2007.

[24] ODVA, "Volume 1: CIP Common," Available: http://www.odva.org/10_2/03_events/03_ethernet-homepage.htm.

[25] ODVA, "Volume 2: EtherNet/IP Adaptation on CIP," Available: http://www.odva.org/10_2/03_events/03_ethernet-homepage.htm

[26] IEC 61784-1, Available at: www.iec.ch.

[27] IEC 61784-2, Available at: www.iec.ch.

[28] M. Blanke, M. Kinnaert, J. Lunze, and M. Staroswiecki, "Diagnosis and Fault-Tolerant Control," 2nd Edition, Springer, 2006.

[29] Ch. Buckl, D. Sojer, and A. Knoll, "FTOS: Model-driven development of Fault-Tolerant automation systems," Proceedings of the IEEE International Conference on Emerging Technologies and Factory Automation ETFA, Bilbao, Spain, September 2010.

[30] R.M. Daoud, H.M. ElSayed, and H.H. Amer, "Gigabit Ethernet for Redundant Networked Control Systems," Proceedings of the IEEE International Conference on Industrial Technology ICIT, Hammamet, Tunis, December 2004.

[31] H.H. Amer, M.S. Moustafa, and R.M. Daoud, "Optimum Machine Performance In Fault-Tolerant Networked Control Systems," Proceedings of the IEEE EUROCON Conference, Belgrade, Serbia & Montenegro, November 2005.

[32] H.H. Amer, M.S. Moustafa, and R.M. Daoud, "Availability of Pyramid Industrial Networks", Proceedings of the Canadian Conference on Electrical and Computer Engineering CCECE, Ottawa, Canada, May 2006.

[33] H.H. Amer and R.M. Daoud, "Parameter Determination for the Markov Modeling of Two-Machine Production Lines," Proceedings of the International IEEE Conference on Industrial Informatics INDIN, Singapore, August 2006.

[34] D.P. Siewiorek and R.S. Swarz, Reliable Computer Systems – Design and Evaluation, A K Peters, Natick, MA, USA, 1998.

[35] B.R. Haverkort, R. Marie, G. Rubino, and K. Trivedi, "Performability modelling: techniques and tools," John Wiley & Sons, 2001.

[36] Official site for OPNET Network Modeler: www.opnet.com

[37] K.S. Trivedi, Probability and statistics with reliability, queuing, and computer science applications, Wiley, NY, USA 2002.

[38] R.M. Daoud, "Wireless and Wired Ethernet for Intelligent Transportation Systems," DSc Dissertation, LAMIH-SP, Universite de Valenciennes et du Hainaut Cambresis, France 2008.

[39] N. Navet, Y. Song, F. Simonot-Lion, and C. Wilwert, "Trends in Automotive Communication Systems," Proceedings of the IEEE, Vol. 93, No. 6, 2005.

[40] K. Ahlstrom, J. Torin, and P. Johannessen, "Design method for conceptual design of By-Wire Control: Two case studies," Proceedings of Seventh IEEE International Conference on Engineering of Complex Computer Systems ICECCS, Skövde, Sweden, 2001.

[41] H. Kirrmann and P.A. Zuber, The IEC/IEEE Train Communication Network, ABB Corp. Res., 2001.

[42] T. Sullivan, The IEEE 1473-L Communications Protocol: Experience in rail transit, Transportation Systems Design, Inc, Oakland, CA, USA.

[43] H. Kitabayashi, K. Ishid, K. Bekki, and M. Nagasu, New train control and information services utilizing broadband networks, 2004.

[44] Train Communication Network, IEC 61375, International Electrotechnical Committee, Geneva, 1999.

[45] Trains reference list, Siemens AG Transportation systems trains, Germany, pp. 41-46.

[46] G. Krambles, J.J. Fox. and W.J. Bierwagen, Automatic train control in rapid transit, 1976.

[47] T. Neiva, A. Fabri and A. Wegmann, "Remote Monitoring of Railway Equipment using Internet Technologies," Laboratory for computer Communications and Applications.

[48] M. Tabbara, A. Rantzer, and D. Nešić, "On controller & capacity allocation co-design for networked control systems," Systems & Control Letters, Vol. 58, Issue 9, September 2009.

[49] R.M. Daoud, H.H. Amer, H.M. Elsayed, and Y. Sallez, "Fault-Tolerant Ethernet-Based Vehicle On-Board Networks," Proceedings of the Conference of the IEEE Industrial Electronics Society IECON, Paris, France, November 2006.

[50] M. Aziz, B. Raouf, N. Riad, R.M. Daoud, and H.M. Elsayed, "The Use of Ethernet for Single On-board Train Network," Proceedings of the IEEE International Conference on Networking, Sensing and Control ICNSC, Hainan, China, 2008.

[51] M. Hassan, S. Gamal, S. Louis, G.F. Zaki, and H.H. Amer, "Fault Tolerant Ethernet Network Model for Control and Entertainment in Railway Transportation Systems," Proceedings of the Canadian Conference on Electrical and Computer Engineering CCECE, Niagara Falls, ON, Canada, 2008.

[52] M. Hassan, R.M. Daoud, and H.H. Amer, "Two-wagon Fault-Tolerant Ethernet Networked Control System," Proceedings of the Applied Computing Conference, Istanbul, Turkey, May 2008.

[53] M. Hassan, G.F. Zaki, R.M. Daoud, H.M. ElSayed, and H.H. Amer, "Reliable Train Network Using Triple Modular Redundancy at the Sensors Level," International Journal of Factory Automation, Robotics and Soft Computing, 2008, pp. 39-44.

[54] D. Dzung, J. Endresen, C. Apneseth, and J. E. Frey, "Design and Implementation of a Real-Time Wireless Sensor/Actuator Communication System," Proceedings of the 10th IEEE International Conference on Emerging Technologies and Factory Automation, ETFA, Catania, Italy, September 2005.

[55] ABB, "Technical Description WISA Wireless Interface for Sensors and Actuators: Planning, installation and commissioning guidelines," March 2009.

[56] R. Steigmann and J. Endresen, "Introduction to WISA: WISA – Wireless Interface for Sensors and Actuators," White paper, ABB, July 2006.

[57] G. Boggia, P. Camarda, V. Divittorio, and L.A. Grieco, "A simulation-based performance evaluation of Wireless Networked Control Systems," Proceedings of the 14th IEEE International Conference on Emerging Technologies and Factory Automation, ETFA, Mallorca-Spain, September 2009.

[58] M. Pinheiro, S. Sampaio, P. Souto, and F. Vasques, "A DHT-based approach for path selection and message forwarding in IEEE 802.11s industrial wireless mesh networks," Proceedings of the 14th IEEE International Conference on Emerging Technologies and Factory Automation, ETFA, Mallorca-Spain, September 2009.

[59] G. Cena, A. Valenzano, C. Zunin, and L. Seno, "Evaluation of Real-Time communication performance in QoS-enabled infrastructure WLANs," Proceedings of the 14th IEEE International Conference on Emerging Technologies and Factory Automation, ETFA, Mallorca-Spain, September 2009.

[60] L. Seno, S. Vitturi, and F. Tramarin, "Experimental Evaluation of the Service Time for Industrial Hybrid (Wired/Wireless) Networks under Non-Ideal Environmental Conditions," Proceedings of the IEEE Conference on Emerging Technologies and Factory Automation ETFA, Toulouse, France, September 2011.

[61] IEEE 802.11 Standard

[62] IEEE 802.15.4 Standard

[63] IEEE 802.15.1 Standard

[64] S.B. Morris, Automated Manufacturing Systems Actuators, Controls, Sensors, and Robotics, McGraw-Hill, 1995.

[65] T.K. Refaat, R.M. Daoud, H.H. Amer, and E.A. Makled "WiFi Implementation of Wireless Networked Control Systems," Proceedings of the 7th International Conference on Networked Sensing Systems INSS, Kassel, Germany, June 2010.

[66] T.K. Refaat, R.M. Daoud, H.H. Amer, M. Hassan, and O.M. Sultan, "Workcell concatenation using WiFi-based Wireless Networked Control Systems," Proceedings of the 17th IEEE International Conference on Electronics, Circuits, and Systems ICECS, Athens, Greece, December 2010.

[67] T.K. Refaat, E.A. Makled, R.M. Daoud, H.H. Amer, and M. Hassan, "Fault-Tolerant Controllers in Adjacent Wireless Networked Control Systems Using 802.11," Proceedings

of the 3rd IEEE International Congress on Ultra Modern Telecommunications and Control Systems ICUMT, Budapest, Hungary, October 2011.

[68]   M.C. Magro and P. Pinceti, "Measuring real time performances of PC-based industrial control systems," Proceedings of the IEEE Conference on Emerging Technologies and Factory Automation ETFA, September 2007.

[69]   T.K. Refaat, M. Hassan, R.M. Daoud, and H.H. Amer, "Ethernet Implementation of Fault Tolerant Train Network for Entertainment and Mixed Control Traffic," **submitted for review** to the International Journal of Factory Automation, Robotics and Soft Computing, December 2011.

[70]   T.K. Refaat, H.H. Amer, R.M. Daoud and M.S. Moustafa, "On the Performability of On-Board Train Networks with Fault-Tolerant Controllers," Proceedings of the IEEE International Conference on Mechatronics ICM, Istanbul, Turkey, April 2011.

[71]   Official site for Cisco Catalyst 3560 Series Switch: http://www.cisco.com/en/US/products/hw/switches/ps5528/

[72]   A. Enteshari and M. Kavehrad, "Transmission strategies for high-speed access over Category-7A copper wiring," Proceedings of the Canadian Conference on Electrical and Computer Engineering CCECE, Niagara Falls, Canada, May 2008.

[73]   T.K. Refaat, H.H. Amer, and R.M. Daoud, "Reliable Architecture for a Two-Wagon Switched Ethernet Train Control Network," Proceedings of the 3rd IEEE International Congress on Ultra Modern Telecommunications and Control Systems ICUMT, Budapest, Hungary, October 2011.

[74]   T.K. Refaat, R.M. Daoud, H.H. Amer, and M.S. ElSoudani, "Cascading Wireless Industrial Workcells," Proceedings of the IEEE International Conference on Mechatronics ICM, Istanbul, Turkey, April 2011.

[75]   Official site for Cisco Systems, Inc: www.cisco.com.

[76]   Official site for Nortel: http://www.nortel.com.

[77]   T.S. Rappaport, Wireless Communications: Principles and Practice, 2nd ed., Prentice Hall, 2002.

[78]   S. Zvanovec, P. Pechac and M. Klepal, "Wireless LAN networks design: Site survey or propagation modeling?" Journal of Radioengineering, Vol. 12, No. 4, Dec 2003.

[79]   Rec. ITU-R M.1225, "Guidelines for evaluation of radio transmission technologies for IMT-2000," 1997, available at: http://www.itu.int/oth/R0A0E00000C/en.

[80]   Cisco Systems, "Channel deployment issues for 2.4-GHz 802.11 WLANS," 2004, http://www.cisco.com/en/US/docs/wireless/technology/channel/deployment/guide/Channel.html.

[81]   T.K. Refaat, R.M. Daoud, and H.H. Amer, "Wireless Fault-Tolerant Controllers in Cascaded Industrial Workcells using WiFi and Ethernet" **submitted for review** to the International Journal of Advanced Manufacturing Technology, Springer, November 2011.

[82]   T.K. Refaat, R.M. Daoud and H.H. Amer, "Fault-Tolerant Controllers in Wireless Networked Control System using 802.11g," Proceedings of the IEEE International Conference on Industrial Technology ICIT, Athens, Greece, March 2012.